FRONTIERS IN NUCLEAR SCIENCE (*)

J. H. HAMILTON
Department of Physics and Astronomy, Vanderbilt University,
Nashville, TN 37235, USA

WALTER GREINER
Institute für Theoretische Physik,
Universität Frankfurt/Main
Frankfurt/Main, West Germany

(Received 23 December 1982)

ABSTRACT — A review is made of some of the frontiers in nuclear research with heavy ions. Recent results from studies of nuclei far from stability, very high spin states and nuclear molecules with $Z = 184$ are given. New applications of nuclear techniques in medicine, positron emission tomography and nuclear magnetic resonance, also are presented.

1 — INTRODUCTION

The last decade has seen the development of exciting new frontiers in basic nuclear science and in the application of nuclear science in important societal problems such as health care and energy. New accelerator facilities which can give beams of heavy ions all the way to uranium with up to 10 and more MeV per nucleon and in some cases over 1 GeV per nucleon are opening up many exciting, new areas in nuclear, atomic and solid state physics, astrophysics, chemistry, materials science, and beyond. From the broad spectrum of basic and applied nuclear science, a few limited examples were selected to illustrate some of the new frontiers and the excitement they are generating. In basic research, examples are drawn from studies of nuclei far from

(*) This paper is based on two talks, one delivered and one prepared for the Third National Physics Conference of the Portuguese Physical Society (Coimbra, June 1982).

the stable ones found in nature, nuclei under conditions of high angular momentum, and the properties of atoms with Z up to 188 and tests of quantum electrodynamics of very strong fields. In applied research, there is again a broad range from uses of heavy ions to initiate the fusion of hydrogen into helium in a fusion energy reactor to nuclear medicine. Within the last several years, new applications of nuclear techniques in positron emission tomography and nuclear magnetic resonance offer the promise of revolutionizing diagnostic medicine. Illustrations of the power of these new techniques are given.

Three sections of this paper were prepared from a talk given at the Third Portuguese National Physics Conference. These sections are intended to be only illustrative and not comprehensive as in a regular review article. The fourth section was prepared for the conference but in the absence of the second author presented only briefly by the first. We have given full attention to the exciting developments in the studies of atoms with Z up to 188 in this combined paper.

2 — SHAPE COEXISTENCE AND SUPER DEFORMATION AROUND $Z = N = 38$

For over two decades after Bohr and Mottelson [1] described collective excitations in nuclei with rotational motions in deformed nuclei and vibrational motions in both spherical and deformed nuclei, the classification of a nucleus as a deformed rotor or spherical vibrator clearly defined its shape and the general features of its structure. Regions of deformation occurred essentially in heavy nuclei where the neutron number is far removed from closed shells. Additional regions of deformation were expected in similar regions labelled one and three (Fig. 1). Near the closed shells or below $N = 50$ where N and Z were never very far from a magic number, nuclei were considered spherical with only a few exceptions and were described by shell or vibrational models.

The discoveries of the coexistence of overlapping low energy states with well deformed and near spherical shapes in both the light mercury nuclei far off stability [2, 3] and in ^{72}Se (refs. 3-5) helped break down the idea that a given nucleus had one fixed shape. The bands built on the different shapes in $^{184\text{-}188}$Hg are shown in Fig. 2. The $2 \rightarrow 0$ energies in the two bands are inversely

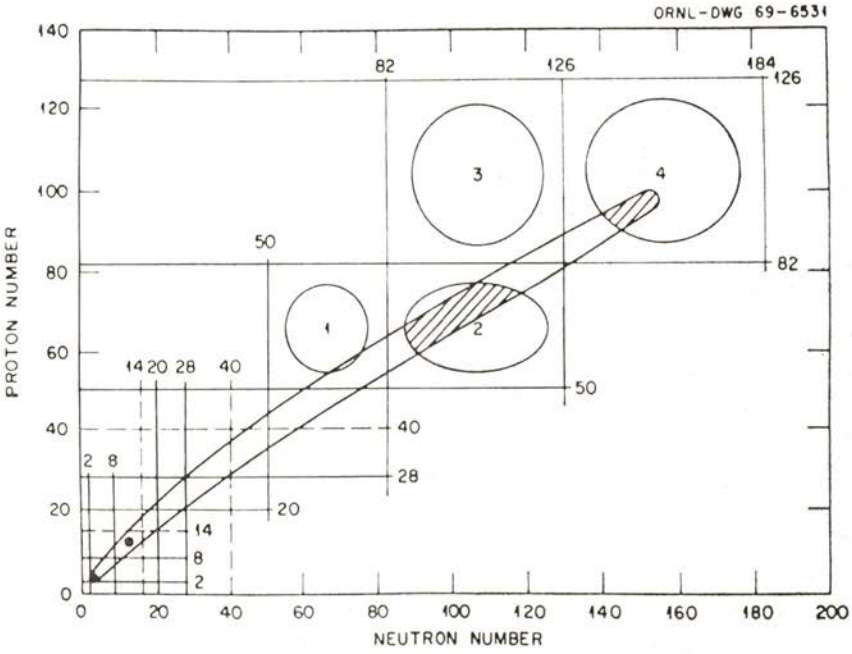

Fig. 1 — An older chart of the nuclides as functions of N and Z with the nuclei in the valley of beta stability inside the ellipse. The closed shells are shown by lines and the known and then predicted new regions of deformation far off stability are identified by circles.

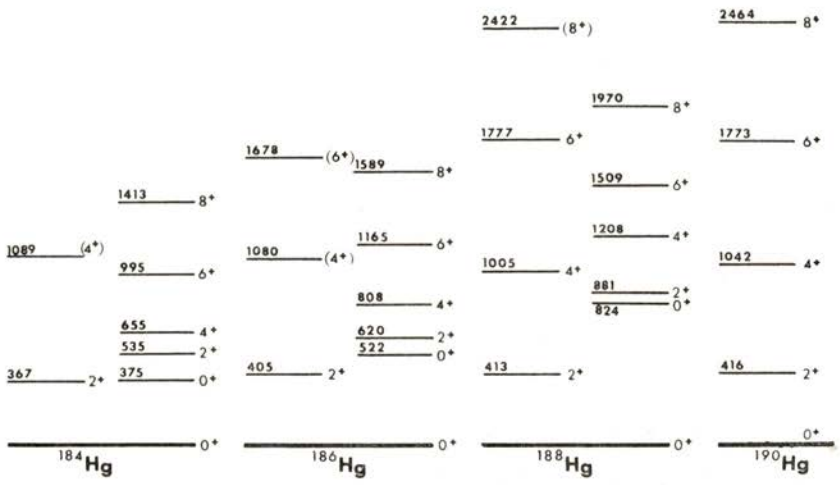

Fig. 2 — Energy levels in $^{184\text{-}188}$Hg where coexisting bands of levels built on different shapes are observed [2, 3].

proportional to the moments of inertia and so show clearly the large differences in deformation in the two bands. Now shape coexistence is reported in many regions of the periodic table including at both low and high spins as can be seen, for example, in numerous papers in the Proceedings of the most recent Conference on Nuclei Far From Stability at Helsingør, 1981.

The A = 60 to 84 region has become an important, new testing ground for many types of nuclear structure models because of the richness of different collective motions and structures which are found in this region and the rapid changes seen in some structures with the addition of only two protons or two neutrons. Some of the variety of different structures and the rapidity of their changes can be seen in an earlier survey of the moments of inertia as a function of the rotational frequency $(\hbar\omega)^2$ for the yrast states in nuclei in this region (Fig. 3). Note the striking difference between ^{68}Ge with its triple forking at 8^+ and two back bends of $\mathcal{J}$ as discovered by de Lima et al. [6] and the single band with forward

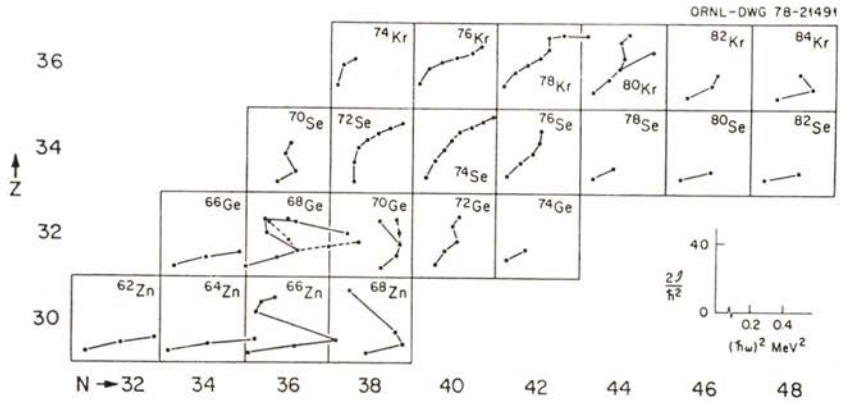

Fig. 3 — Moments of inertia for the yrast cascades in A = 60-80 region [5].

bend in ^{72}Se. The first nucleus studied to high spin was ^{72}Se (ref. 4) and its strong forward bend of $\mathcal{J}$, very like the forward bends of $\mathcal{J}$ seen [2, 3] in $^{184\text{-}188}$Hg, was similarly interpreted in terms of shape coexistence [3-5]. While there is definite exper-

imental evidence [7, 8] supported by theoretical calculations [7, 9] that the low lying 0_2^+ states in $^{70,72}_{32}$Ge indeed have much larger deformations than their ground states as in $^{72,74}_{34}$Se, they have no well developed rotational bands built on the 0_2^+ states. This was considered by some as a serious problem for the shape coexistence picture.

Recent studies [10] of ^{74,76}Kr have illuminated the origin of the shape coexistence in this region and given evidence for super deformation of the ground states where both N and Z are at or near 38. The $2_1^+ \rightarrow 0_1^+$ energy does not indicate super deformation in $^{74}_{36}Kr_{38}$. The origin of the masking of the strong deformation now is understood in terms of the interaction of two close lying 0^+ states [10]. A similar masking is now understood to occur in the light Pt isotopes. Simultaneously, Möller and Nix [11] carried out calculations that predicted that nuclei in this region around $N = Z = 38$ should have the strongest ground state deformation of any nuclei, with $\beta \sim 0.4$. Likewise, the recent analysis of the levels of $^{74\text{-}80}$Kr in the collective potential energy surface approach of the Frankfurt group [12] indicate shape coexistence and large deformations in ^{74,76}Kr. New studies in the Sr nuclei [13, 14, 15] support this conclusion. Indeed, we have found experimentally [10] and independently predicted theoretically [11] a new region of strong deformation. The understanding of the origin of this deformation gives insights into nuclear shape coexistence in a wide range of different masses.

Our studies of the light Kr isotopes provide the clues to understanding this region. The $B(E2; 2 \rightarrow 0)$ for ^{78,80,82,84,86}Kr were measured by Sakamoto et al. [16]. They found nearly a factor of 10 increase in $B(E2)$ strength in going from $N = 50$, $^{86}_{36}$Kr, $B(E2; 2 \rightarrow 0) = 6.5$ spu to ^{78}Kr where it is 51.8 spu. This suggests the onset of large collective effects possibly associated with deformation. However, the $2 \rightarrow 0$ energies (455-617 keV) do not suggest large deformation.

We investigated the levels in ^{76}Kr and our results are shown in Fig. 4 (ref. 10). Note the dominance of rotational-like band structures. We measured the $B(E2)$ strengths of the transitions from the 4^+ to 10^+ levels by Doppler-shift, line-shape analysis [10]. Both singles and concidence spectra line shapes were analized.

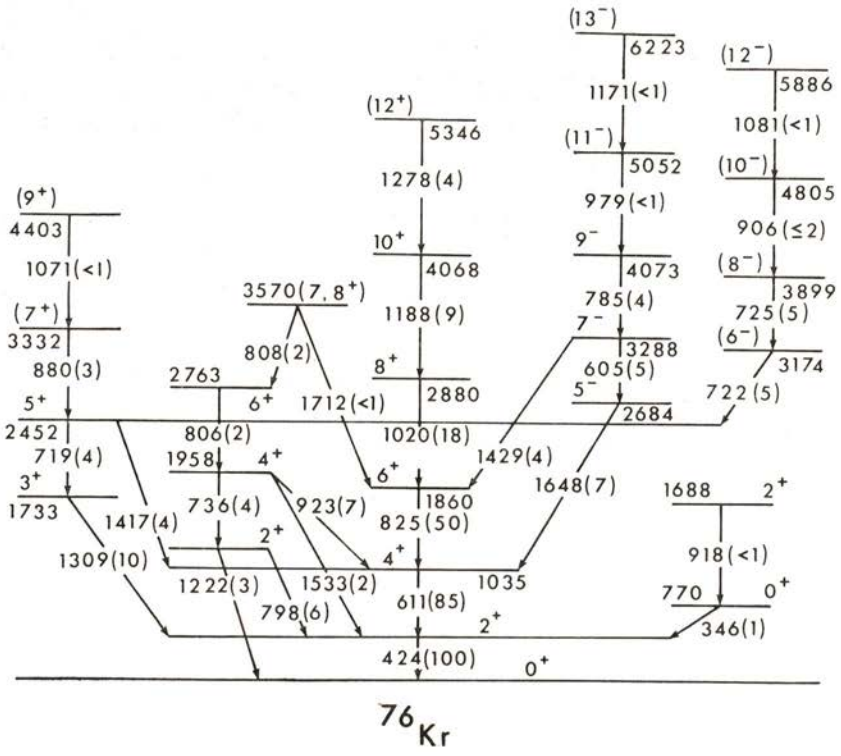

Fig. 4 — Energy levels in ^{76}Kr from in-beam studies [10].

The results are given in Table I along with similar results more recently obtained by Winter et al. [17]. The B(E2)'s show surprisingly large collective strength — the largest of any nucleus in this region. For comparison the $B(E2)_{exp}/B(E2)_{sp}$ for the $2 \rightarrow 0$ and $4 \rightarrow 2$ transitions in $^{68, 72}$Ge are of the order of 10-20. These data provide strong evidence for large collective effects associated with nuclear deformation. From the 2^+ to 10^+ level, the B(E2) values generally follow the gradual increase expected in a rotational model in sharp contrast to the rapid increase in B(E2) in a vibrational model.

Note in ^{76}Kr that the energy of the first excited, 0_2^+, level has continued to drop sharply relative to the 0_1^+ ground state as N decreases analogous to the similar sharp drops seen in Ge and Se nuclei around N = 40. But there is no rotational band built on it as in ^{72}Se. The only feeding to the 0_2^+ level is from a 2^+

TABLE I — Measured mean lives and extracted B(E2) values [10, 17] for transitions in ^{76}Kr.

E_γ (keV)	$I_i \rightarrow I_f$	τ_{mean} (ps) (ref. 10)	τ_{mean} (ps) (ref. 17)	τ_{mean} (ps) Average	$B(E2)/B(E2)_{sp}$
424	$2^+ \rightarrow 0^+$	53(7) †	35(3) ††	40(5)	78(9)
611	$4^+ \rightarrow 2^+$	5.0(20)	3.5(10)	4.2(10)	120(30)
825	$6^+ \rightarrow 4^+$	1.25(12)	0.9(2)	1.12(10)	99(10)
1020	$8^+ \rightarrow 6^+$	0.30(3)	0.32(4)	0.31(3)	125(12)
1188	$10^+ \rightarrow 8^+$	0.14(2)	0.18(4)	0.15(2)	120(20)
1278	$(12^+) \rightarrow 10^+$	0.24(5) *			52(11) *

* Composite state plus feeding lifetime and composite B(E2) compared to single particle values.

† E. NOLTE et al., *Z. Phys.* **A268**, 267 (1974).

†† J. KEINONEN et al., *Nucl. Phys.* **A376**, 246 (1982).

level at 1688 keV. Note the $2^+ \rightarrow 0_2^+$ energy of 917 keV is more than twice the $2_1^+ \rightarrow 0_1^+$ energy of 424 keV. This is in sharp contrast to ^{72}Se where these two energies are the reverse, eg., the $2^+ \rightarrow 0_2^+$ energy is low compared to the $2_1^+ \rightarrow 0_1^+$ energy. A $(2^+) \rightarrow 2^+ \rightarrow 0_2^+$ cascade (882-917 keV γ rays) is seen in UNISOR studies [18] of the decay of ^{76}Rb. All these data indicate that something different and unsual is happening in ^{76}Kr.

We carried out a similar study of the energy levels in ^{74}Kr (ref. 10). The moments of inertia for $^{74\text{-}80}$Kr are shown in Fig. 5. One can see from Fig. 5 that at low spin, $\mathcal{J}$ of each band becomes larger when going from N = 44 to N = 38, except for ^{74}Kr where the point corresponding to the $2 \rightarrow 0$ energy in ^{74}Kr strongly deviates as first noted by Funke et al. [19]. This tendency also is seen in ^{76}Kr to a lesser degree. These nuclei exhibit forward bends in $\mathcal{J}$ above the 2_1^+ states analogous to those in $^{72,\,74}Se_{38,\,40}$ which were interpreted (refs. 3, 4) in a shape coexistence picture with bands built on the ground and 0_2^+ states of quite different deformations. All the above data led to the suggestion that the ground state of ^{76}Kr is well deformed and the 0_2^+ level is associated with a near-spherical shape [10], in contrast to the reverse situation in $^{72,\,74}$Se. A similar situation should be occurring in ^{74}Kr.

How can we understand large ground state deformation but relatively small $\mathcal{J}$'s extracted from the relatively large $2 \rightarrow 0$ energies in $^{74\text{-}76}$Kr? The relatively large $2 \rightarrow 0$ energies and corresponding small $\mathcal{J}$ in $^{74, 76}$Kr, which make these nuclei look less deformed than they really are, can arise from an interaction between the 0_1^+ deformed ground states and higher states such as the 0_2^+ states to push down the 0_1^+ energies. Shape coexistence for N ~ 38 nuclei is related to the number of protons which delicately controls whether a deformed shape or near-spherical shape is lowest in this region. Our $^{74, 76}$Kr data give evidence that their ground states have remarkably large deformation.

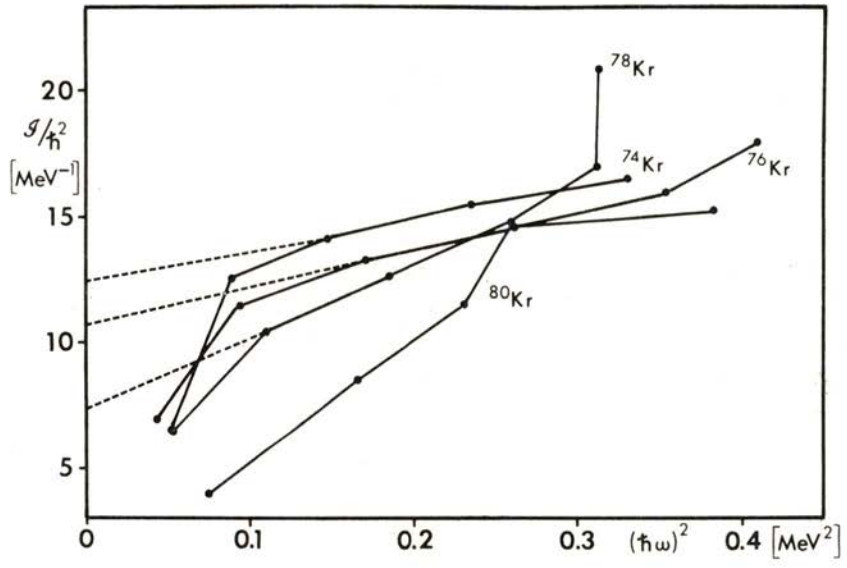

Fig. 5 — The moment of inertia of the yrast cascades are shown. The dashed lines correspond to an extrapolation back to low spin of a Harris parametrization of the states with I = 6 - 10 where $\mathcal{J}$ is linear [10].

The origin of strong deformation and shape coexistence in this region can be attributed to the gaps in the single-particle spectrum seen in Fig. 6 at N (or Z) = 40, δ ~ 0, and N (Z) = 38, δ ~ 0.3, that stabilize the nuclear shape. Evidence for the spherical subshell closure around N = 40 is found when Z is close or equal

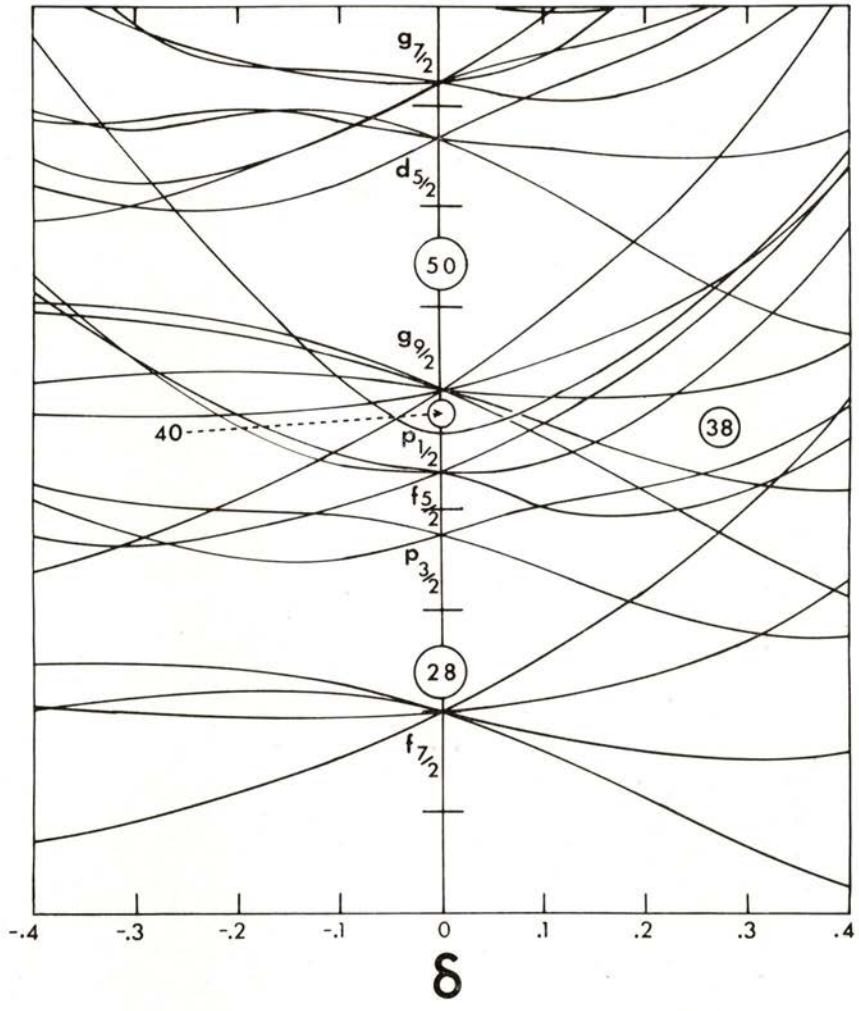

Fig. 6 — The Nilsson single particle spectrum for protons. Note the gap at N = 38 for large deformation. The neutron spectrum is similar.

to 28 or 50, or around Z = 40 when N ~ 28 or 50 because then the protons (neutrons) prefer a spherical shape, as seen for example in $^{66}_{28}Ni_{38}$ ($^{90}_{40}Zr_{50}$). However, as Z moves away from 28 or 50 the level density for a spherical shape becomes very high and the minimum of the proton deformation energy moves to deformed shapes and similarly for the neutrons which have almost identical

single-particle levels. Away from Z (N) = 28 and 50 closed shells, maximal deformation is expected at N (Z) ~ 38. However, the deformed state can coexist with a nearly spherical configuration in a delicate balance. Which one is lower depends on the proton number. For $^{70,72}_{32}Ge_{38,40}$ and $^{72,74}_{34}Se_{38,40}$ the coexistence of nearly spherical ground states with deformed 0^+_2 states has been reported [3, 5, 7] as noted earlier. In ^{72,74}Se, the deformed band becomes yrast at I ~ 2 — 4 because of its lower rotational energy. For the Ge isotopes, the bands built on the two different shapes are not well developed and so not seen because of the smaller deformation (two protons less than Se). In the Kr isotopes, the 36 protons favor deformation even more.

To quantify our interpretation, we analyzed [10] the Kr yrast bands in a two-band mixing model. For $I \gtrsim 6\hbar$, where $\mathcal{J}$ is nearly linear, we considered the yrast levels to be purely deformed. The up bends above 8^+- 10^+ (Fig. 5) are related to the alignment of a $g_{9/2}$ proton pair. The position of the unperturbed deformed levels were determined by extrapolating the linear part of $\mathcal{J}(\omega^2)$ down to $\omega = 0$. This corresponds to a Harris or variable moment of inertia (VMI) parametrization of the deformed g bands. The extracted unperturbed $2 \rightarrow 0$ energies in the deformed ground bands are 200 and 237 keV in ^{74,76}Kr, respectively. By scaling the unperturbed $2 \rightarrow 0$ energy by $A^{5/3}$, one may compare the deformation of ^{74}Kr to that of strongly deformed ^{240}Pu with one of the lowest $2 \rightarrow 0$ energies known. The 200 keV transition in ^{74}Kr would correspond to 28 keV in ^{240}Pu compared with its actual value of 43 keV (see Fig. 7). This is an unusually large ground-state deformation, slightly larger than the "super deformation" recently reported for ^{100}Sr with its scaled 30 - keV 2^+_1 (Fig. 7) energy [20]. Such interaction of two 0^+ levels and their splitting may have masked strong ground-state deformation in other regions. Indeed, recent analysis indicates that this is clearly happening in the light platinum isotopes, too.

These data extend our understanding of the coexistence of different nuclear shapes first proposed in ^{72}Se. However, in ^{74,76}Kr the roles of the near-spherical and deformed minima are reversed with the ground states well deformed and the excited 0^+_2 states associated probably with near-spherical minima. The present data give evidence for large ground-state deformation in these light Kr isotopes [10]. This interpretation for the N = 38 and 40 Kr nuclei

supports the expectation that at these neutron numbers as the proton number approaches the middle between Z = 28 and 50 closed shells, the protons can drive a nucleus with a pair of $g_{9/2}$ neutrons toward deformation. Recently Möller and Nix [11] calculated nuclear masses and ground state shapes for 4023 nuclei from $^{16}0$ to $^{279}112$ with a Yukawa-Plus-Exponential Macroscopic Model and a folded Yukawa single-particle potential. Their calculations [11] predict that nuclei with both N and Z at or near 38 should be among the most strongly deformed ones in nature, with $\beta \sim 0.4$. The ^{74,76}Kr data [10] support their calculations.

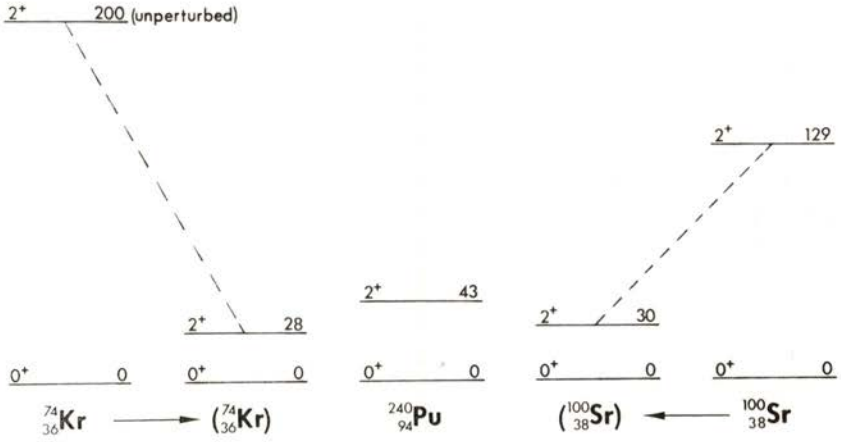

Fig. 7 — Comparison of the $2_1 - 0_1$ energies in $^{74}_{36}Kr_{38}$ and $^{100}_{38}Sr_{62}$ scaled by $A^{5/3}$ to compare with the very well deformed ^{240}Pu.

Potential energy surfaces have recently been calculated for $^{76-80}$Kr by the Frankfurt group [12]. The ^{76}Kr surface is shown in Fig. 8. Two minima are seen, one at large deformation and one near spherical. There is mixing, but the ground state wave function is centered in the deformed minimum with large β and the 0_2^+ wave function in the near spherical one. The low lying levels and their B(E2)'s are nicely reproduced by the fits. For ^{78,80}Kr the surfaces show the nuclei are soft to γ deformation.

Further support for the importance of deformation when N(Z) = 38 and Z(N) is well removed from a closed shell come from the lightest and heaviest Sr nuclei far from stability [13, 14, 15].

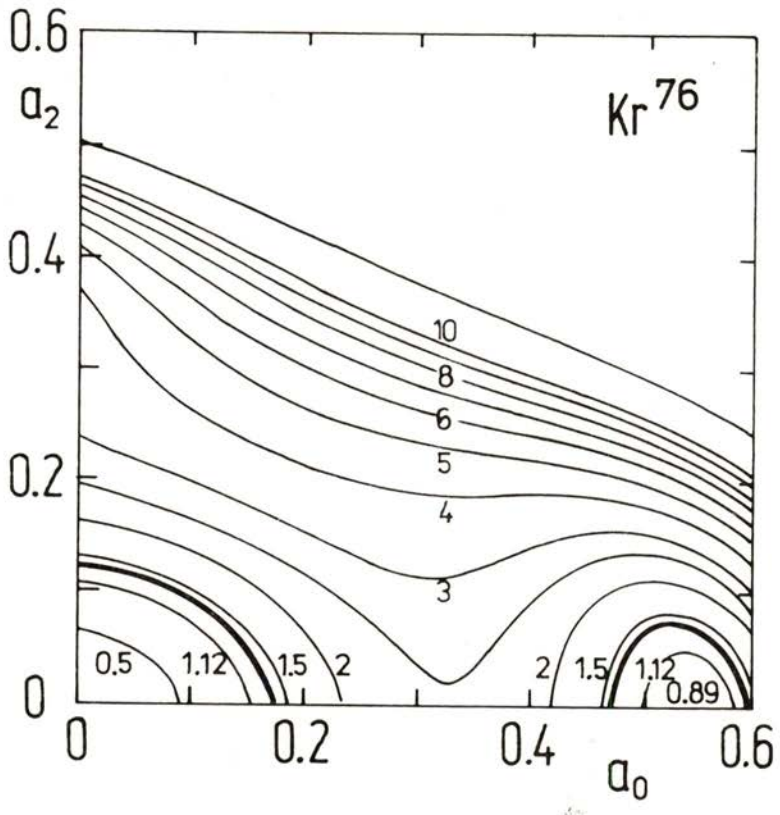

Fig. 8 — Potential energy surface for ^{76}Kr (ref. 12). Note two minima at large deformation and at zero deformation. Note $a_0 \sim \beta$.

In Fig. 9 is shown the yrast levels of $^{80}_{38}Sr_{42}$ obtained from a recent in-beam study (ref. 13) at the new Holifield tandem. The reaction $^{32}S + {}^{51}V$ was carried out with terminal voltages of 16-19 MeV. One sees (Fig. 9) that the $2 \rightarrow 0$ energy continues to drop to the lowest energy then known for any nucleus in the A = 80 region. This sharp drop in the $2 \rightarrow 0$ energies indicates that the Sr nuclei are moving toward large ground-state deformation in $^{76}_{38}Sr_{38}$ as N decreases toward N = 38 with the 38 protons strongly supporting deformation, too. To search for ^{78}Sr, ^{58}Ni was bombarded with ^{24}Mg at the Holifield tandem [14]. A neutron multiplicity technique was used to pick out the (2p, 2n) reaction to ^{78}Sr from other four particle reaction channels. From an initial analysis of only our

(n, γ) spectra, wrong low energy γ rays were assigned as the 0-2-4 cascade. Our $(2n, \gamma)$ data agree with the independent work of Lister et al. [15] who used neutron and particle detectors to

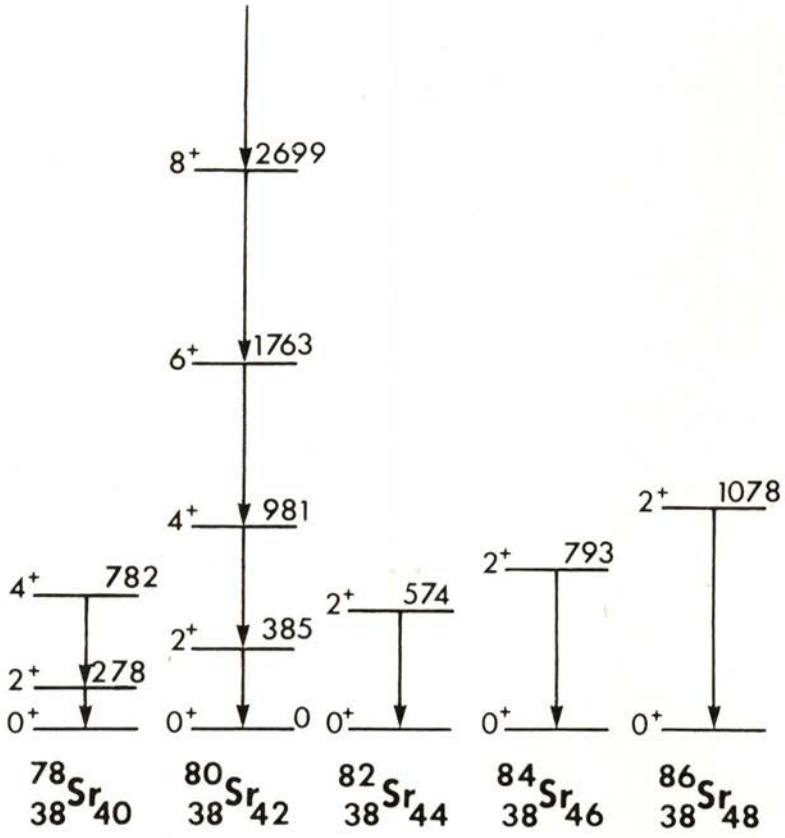

Fig. 9 — Levels of ^{80}Sr seen in the reaction $^{32}S + ^{51}V$ and of ^{78}Sr in the reaction $^{24}Mg + ^{58}Ni$ at the Holifield tandem [13, 14] are compared with the $2 \rightarrow 0$ energies in the heavier nuclei.

identify ^{78}Sr for the first time. Their lifetime measurements also confirm the large deformation. Thus, there is a continued increase toward large deformation at $N = 38$ in the light Sr nuclei.

The sudden onset of strong deformation also has been reported in ^{98}Sr (refs. 21, 22) and "super" deformation subsequently in

^{100}Sr (ref. 20). The origin of this deformation was related [20] to a gap at N = 60 in the neutron Nilsson levels. The potential energy surfaces calculated for the Sr nuclei show minima at large deformation for both prolate and oblate shapes for N = 60 and 62, which are not present for N < 60 (Fig. 10). The experimental data

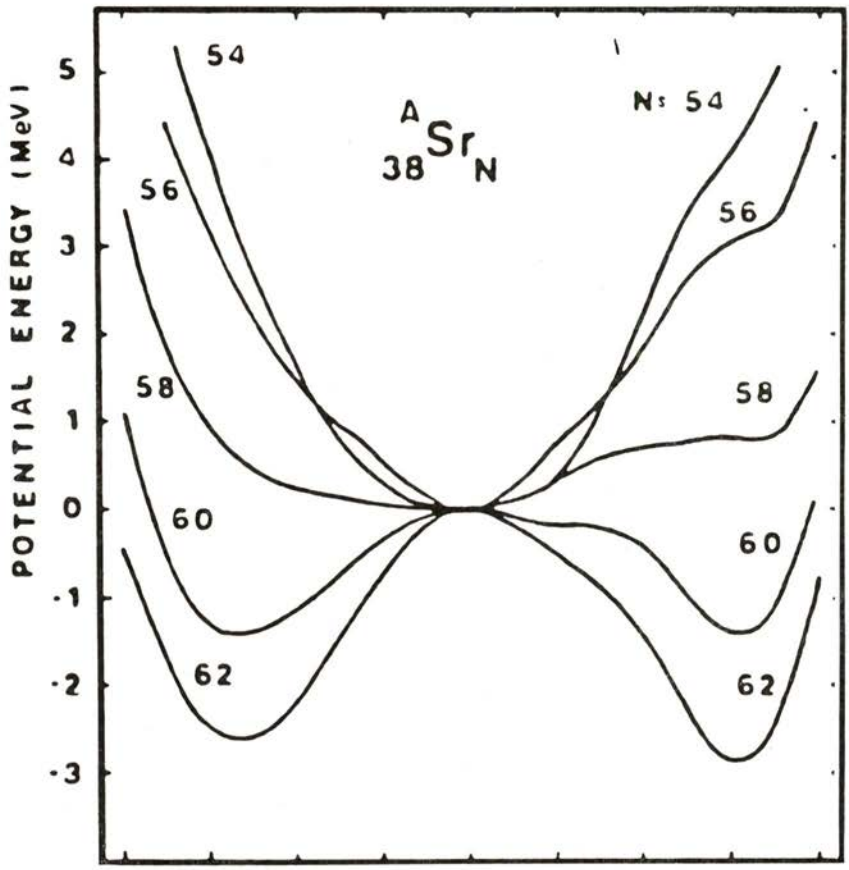

Fig. 10 — Potential energies calculated for Sr nuclei [20].

favor prolate deformation. Now we see this N = 60 gap can be strongly reinforced by the gap at Z = 38 at large prolate deformation. The reinforcement of these two gaps at similar large

prolate deformation is undoubtedly the cause of the sudden large deformation in $^{98, 100}$Sr just as when both N and Z are near 38 they reinforce each other to give unusually large deformation in the $^{74, 76}$Kr ground states. The importance of the gap at Z = 38 in deformation in this region is seen in that as one goes away from Z = 38 the deformation begins to decrease for the N = 60 and 62 nuclei, e.g., the 2_1-0_1 energies are 129.2, 151.9, and 192.2 keV for N = 62 $^{100}_{38}$Sr, $^{102}_{40}$Zr, and $^{104}_{42}$Mo (refs. 20, 23, 24).

Thus, we have found experimentally and supported by theoretical calculations two new regions of strong deformation; one around Z = N = 38 and the other for Z = 38, N $\geq$ 60.

3 — NUCLEI UNDER CONDITIONS OF RAPID ROTATION

What happens to a nucleus at high spins is another of the major areas of nuclear structure research today as evidenced by the several recent international conferences in this field. Theoretical work of Bohr and Mottelson [25] developed for the deformed rare earth nuclei, indicates that as the angular momentum of a deformed nucleus becomes high the nucleus can carry angular momentum more efficiently by the alignment of the spins of pairs of nucleons along the rotation axis. At some spin one ends up with a phase transition so that all the angular momentum is carried in this manner by an oblate shaped nucleus. This occurs around 50 $\hbar$ in rare earth nuclei. At still higher angular momentum, the nucleus may go to a super deformed prolate shape before fission. In this paper we present evidence for the importance of collective rotations and alignment of pairs of particles to record energies in relatively light nuclei around A = 70 and possible evidence for the break off of the rotations and the phase transition around 50 $\hbar$ in ^{158}Er.

Here we describe two new approaches to study high spin states — partial fusion reactions and neutron multiplicity experiments. Here we will describe only two recent experiments to illustrate the new insights being gained. Another important, new advancement is the spin ball spectrometers developed at the Holifield Heavy Ion Laboratory and Max Planck Institute, Heidelberg. In these devices one has a large array of 70 or more NaI detectors that cover essentially a 4 π solid angle to measure

all the γ-rays emitted. Results are just being reported from these systems [26]. The spin ball with a Ge(Li) detector was used to see discrete states in ^{158}Er to spin 40 $\hbar$ and above [26].

3.1 — *Two Discontinuities of $\mathcal{J}$ at High Spin in ^{74}Kr*

Two discontinuities of the moments of inertia, $\mathcal{J}$, of the yrast cascades in ^{158}Er and ^{160}Yb (refs. 27, 28), and very recently a third and possibly higher discontinuity of $\mathcal{J}$ in ^{158}Er (refs. 26, 29, 30) have provided evidence for the persistence of collective rotations and the alignment of individual pairs of quasiparticles to much higher spins than previously thought for deformed rare earth nuclei. As discussed in the previous section, recent evidence for strong ground state deformation was reported in ^{74,76}Kr based on data for states with $I^{\pi} \lesssim 10^{+}$ (ref. 10). With a newly developed neutron multiplicity technique [31] the yrast cascade in ^{74}Kr has been observed [32] to the highest spin reported for a medium-light nucleus, tentatively 20^{+}. Two discontinuities were observed in $\mathcal{J}$ of the yrast cascade in ^{74}Kr.

Backbending of $\mathcal{J}$ has been observed a 8^{+} in ^{68}Ge (ref. 6) and ^{80}Kr (ref. 33) with bands built on three 8^{+} states in ^{68}Ge and two 8^{+} states in ^{80}Kr. These two discontinuities at 8^{+} were interpreted as the crossing of rotation aligned bands built on both proton and neutron $(g_{9/2})^2$ configurations in ^{68}Ge. A similar interpretation is made [33] for ^{80}Kr.

The levels of ^{74}Kr were studied via the reaction ^{58}Ni (^{19}F, p2nγ) ^{74}Kr at 66-68 MeV with > 99 % enriched, thick targets. A recently developed neutron-multiplicity-γ coincidence technique [31] was essential to separate the weak neutron evaporation channel to ^{74}Kr from the competing charged particle channels. Four large liquid scintillator neutron detectors especially designed to cover most of the forward 2π solid angle were used to gate the γ-ray spectra. The overall neutron efficiency of about 30 % made it possible to apply this technique not only to (n, γ) and (n, n, γ) coincidences, but also to (n, γ, γ) measurements, angular distributions, and recoil distance lifetime measurements.

The level scheme of ^{74}Kr was known to 8^{+}. In Fig. 11 is shown the levels established on the basis of our n - γ - γ and

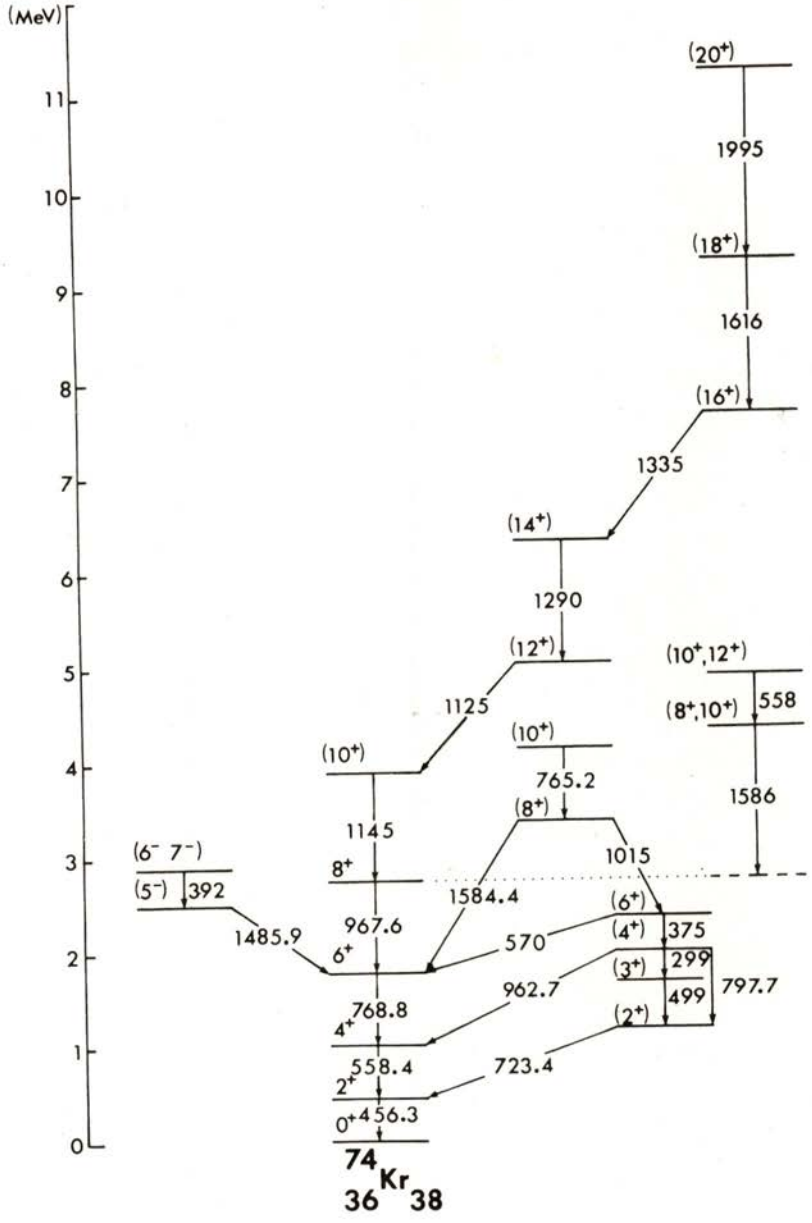

Fig. 11 — Levels in ^{74}Kr established from in-beam, neutron - γ coincidence studies [32, 34].

n - $\gamma(\theta)$ coincidence measurements with a beam energy of 66.5 MeV using a thick target and List-mode technique [32]. States up to a tentative 20^+ state were established. The multipolarities and mixing ratios of the γ - rays were deduced from an angular distribution measurement at the same energy. A γ - ray yield function and $\gamma(\theta)$ data and spectra obtained by gating with one and two neutron events and χ^2 fitting procedure led to the spin assignments displayed in Fig. 11.

In Fig. 12 is shown a plot of the angular momentum $I(\omega)$ as a function of ω where $\hbar\omega = E\gamma\ ((I+1) \rightarrow (I-1))/2$ for our data for ^{74}Kr and other recent results for ^{76,78}Kr (refs. 10, 34). There are three discontinuities seen in $I(\omega)$ for ^{74}Kr. As discussed earlier, the break at 2_1^+ is interpreted as arising from an interaction of the strongly deformed 0_1^+ ground state and a low lying 0_2^+ near-spherical excited state to push down the 0_1^+ energy (and enlarge the $2_1^+ \rightarrow 0_1^+$ energy) [10]. In both ^{74}Kr and ^{78}Kr there are very similar discontinuities in $I(\omega)$ and correspondingly in $\mathcal{J}$ above 10^+. There is only a slight up bend of I in ^{76}Kr. However, in ^{80}Kr two 8^+ and 10^+ states are seen and are interpreted as the crossing of a two quasiparticle rotational aligned band with $(g_{9/2})^2$ protons. In ^{74}Kr two 8^+ and 10^+ levels also are seen. The branching ratios and energies indicate the 8_2^+ and 10_2^+ levels form a band with the yrast 12^+ and (14^+) levels that cross the ground band above 10^+. This is in contrast to ^{80}Kr where the 8_1^+ and 10_1^+ levels are the two quasiparticle rotation aligned states. This first band to cross the ground band is interpreted as a two quasiparticle $(g_{9/2})^2$ configuration, but it is not definite whether it is a proton or neutron configuration.

The second discontinuity of $\mathcal{J}$ occurs above 14^+ with the (16^+), (18^+), and tentative (20^+) states showing similar alignment. Their extra alignment is about the same as the extra alignment in the first band, 2-3 units. No such break in I is seen in the tentatively assigned 16^+ level in ^{78}Kr (ref. 35) which has 4 more neutrons. These data suggest a blocking effect of the extra neutrons and indicate at least two of the four quasiparticles in the highest band in ^{74}Kr are neutrons. In summary, these data provide the first evidence for a second high spin discontinuity

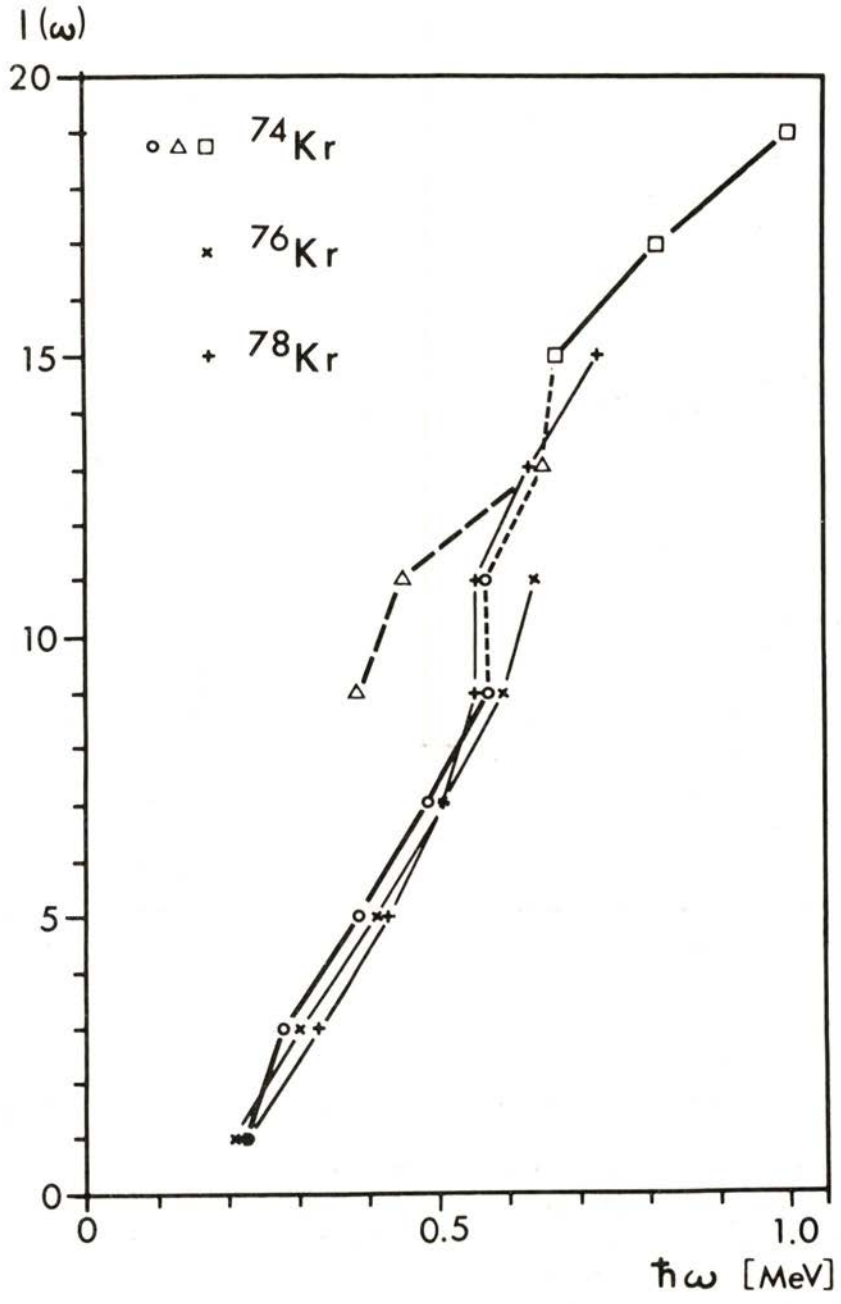

Fig. 12 — Plot of the angular momentum I (ω) as a function of ω (ref. 32).

in $\mathcal{J}$ in a medium-light nucleus and that collective rotations and the alignment of individual two quasiparticle configurations continue to very high energies in this region.

3.2 — *Third and Higher Discontinuities of $\mathcal{J}$ at High Spin in ^{158}Er*

The partial fusion reaction, PFR, in which a fast p, d, or t is emitted in the forward direction followed by the fusion of the remaining part of the projectile is a very promising new way to study nuclei at very high angular momentum. Yamada et al. [35, 29] have studied this reaction by bombarding $^{150, 154}Sm$ with 167 MeV ^{14}N from the Oak Ridge Cyclotron ORIC. The evaporation p, d, t are separated in energy from those from PFR. By gating on the fast p, d, t, the gamma ray multiplicity was measured in the ^{14}N reactions on ^{154}Sm that lead to $^{157\text{-}159}Er$. The ^{158} reaction was more than 50 % of the observed PFR and the gamma-rays from the decay of states to over 40^+ were observed in ^{158}Er.

As shown in Fig. 13, the gamma ray multiplicity is constant as a function of the spin of the yrast states to as high as statistics allow measurement, spin 26, for all three reactions p, d, t that lead to ^{158}Er. A similar multiplicity was measured for the reactions leading to $^{157, 159}Er$. These data indicate no side feeding below $I = 28$. The average M_γ is 31. This is the highest M_γ presently observed. The mass distribution of the residual nuclei also is appreciably more narrow than that for compound nuclear reactions. Both of these data indicate that the PF reactions in which p, d, or t are emitted are associated with a narrow, high angular momentum window [35]. The deduced average angular momentum transferred is 63 $\hbar$ which is comparable to the critical angular momentum l_{cr} predicted for the fusion of ^{13}C and ^{154}Sm.

With this high, narrow l window, the PF reaction should be a very useful tool to study nuclei at high angular momentum. Further support for this is seen in our ^{158}Er studies. In our second ^{158}Er experiment, the same PF reaction was studied with three large, well collimated NaI detectors to obtain an E_γ - E_γ correlation spectrum [29]. The E_γ - E_γ correlation method is a powerful method. To show that it is useful with NaI detectors we carried out very extensive Monte Carlo simulation calculations. These

calculations show that indeed with the order of one to five million events if the background is reasonably low, one can easily study the valley to quite high spins, of the order of 50 $\hbar$.

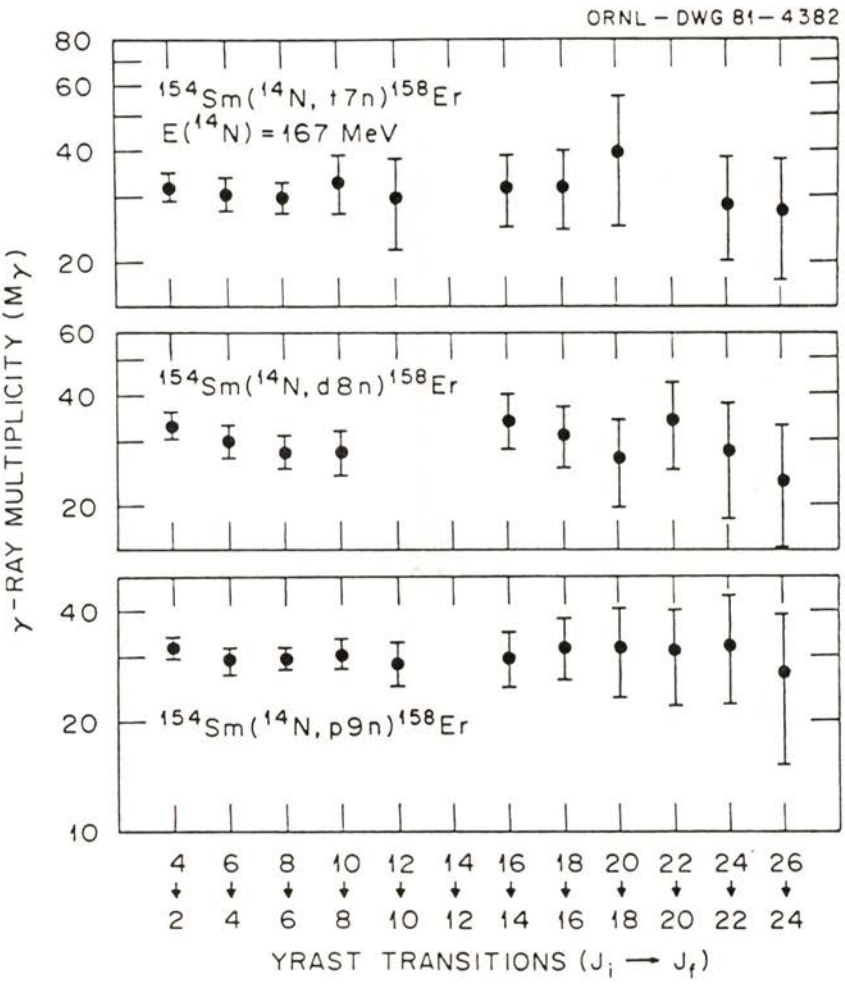

Fig 13 — Measured γ-ray multiplicities in ^{158}Er from PF reactions [35].

The measured and simulated spectra reproduced the known first three backbends of $\mathcal{J}$ in ^{158}Er very nicely. The third backbend

at 1.1 MeV was in fact observed in our data (see Fig. 14) prior to its observation from discrete gamma-ray energies [30]. These data with the Copenhagen iteration method applied to subtract

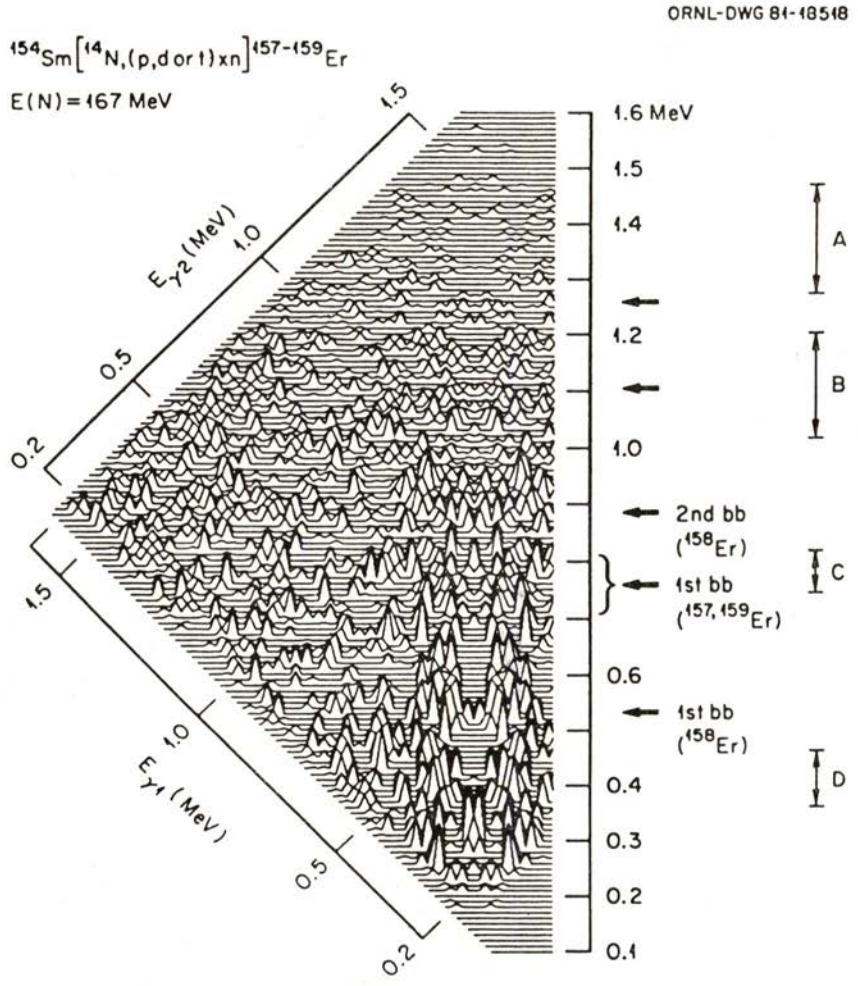

Fig. 14 — E_γ - E_γ correlations in $^{157-159}$Er (ref. 29).

background are from five million events as compared with the 50 million required for Ge (Li) work. The difference in numbers of events required to obtain significant spectra is the essentially

five times higher photo peak efficiency for NaI compared to Ge (Li) detectors and the fact that the PF reactions lead to a high l-window so that many of the side feeding γ rays at lower spins are not present, e.g., the background is much reduced. Note in addition to the third backbend of $\mathcal{J}$, one sees evidence for other bridges at 1.24 and perhaps 1.46 MeV (ref. 29). These bridges are in reasonable agreement with Cranked Shell Model calculations of the next crossings produced from the alignment of the next pairs of quasiparticles [36]. The most important information from these data is the observation that the valley continues to an energy of 1.46 MeV. This valley indicates the continuation of collective excitations to this energy – the highest energy observed to date. These data support the continuation of collective motion up to a spin about $48\,\hbar$. The breakoff of the valley above 1.46 MeV can be the signal for the predicted change of phase from superfluid to normal states associated with a quenching of the pairing field [25]. This is predicted to lead to a change to an oblate shape where the angular momentum is carried by pairs of aligned particles. As discussed in more detail in another paper (Yamada and Hamilton) [29], we believe these data provide evidence for this phase change and that the change is rather sudden.

In summary, these are but two examples of nuclear research that is probing the structures of nuclei at high angular momentum. They show that indeed such studies are important from light to heavy nuclei and are providing us with fascinating new insights into how nucleons behave individually and collectively under extreme conditions of rotation.

4 — NEW CONCEPT OF THE VACUUM AND NUCLEAR MOLECULES WITH $Z = 184$

Since the days of the early Greek natural philosophers our view of the physical world has been dominated by certain paradigms, i.e. specific pictures, for selected physical entities. Such entities are space, time and matter as the basis of natural philosophy or, more specifically, of physics. Therefore, it is no surprise that our conception of the "vacuum", intimately connected with the picture of space, time and matter, ranges among the most

fundamental issues in the scientific interpretation of the world. This section draws upon earlier reviews of this field [37, 38].

The picture of the vacuum has undergone perpetual modifications during the last twenty-five centuries as the available technologies have changed; often old, abandoned ideas have been resurrected when new information became accessible. Many aspects of today's conception of the vacuum date back to the ancient Greek philosophy, but have only recently been established by modern experiments.

Over the centuries many different conceptions of the vacuum were developed by scientists, different vacua as carriers for different kinds of physical phenomena. We mention Newton's absolute space, on which the hypothesis of the vacuum as an elastic medium, the "ether", is based. It was developed in the early 19th century when the wave nature of light had been firmly established — in close analog to the theory of elasticity. In Einstein's theory of relativity and gravity the absolute space and the "ether" were abandoned and replaced by a bundle of inertial frames.

Quantum mechanics and quantum field theory, finally, laid the grounds for our present conception of the nature of the vacuum. In today's language, the vacuum consists of a polarizable gas of *virtual* particles, fluctuating randomly. It is found that, in the presence of strong external fields, the vacuum may even contain "real" particles. The paradigm of "virtual particles" not only expresses a philosophical notion, but directly implies observable effects:

1) The occurrence of spontaneous radiative emission from atoms and nuclei can be attributed to the action of the fluctuations of the virtual gas of photons.
2) The virtual particles cause effects of zero-point motion as in the Casimir effect. (Two conducting, uncharged plates attract each other in a vacuum environment with a force varying like the inverse fourth power of their separation.) Hawking's effect of pair formation by a collapsing body may also be understood as a gravitational Casimir effect.

3) The electrostatic polarizability of the virtual fluctuations can be measured in the Lamb shift and Delbrück scattering.

However, the most fascinating aspect of the vacuum of quantum field theory, which will be discussed here, is the possibility that it allows for the creation of real particles in strong, time-independent external fields. In such a case the normal vacuum state is unstable and decays into a new vacuum that contains real particles. This, in itself, is a deep philosophical insight. But it is more than an academic problem, for two reasons: first, very strong electric fields are available for laboratory experiments that are presently in progress; second it can be shown that the quantum theory of interacting fields may be constructed from the vacuum-to-vacuum amplitude W (J) of a quantized field in the presence of an arbitrary external source J. Effects that occur in strong external fields may, therefore, in some way be carried over to strongly coupled, interacting fields as they form the basis of the strong and superstrong interactions. Only recently have extensive theoretical studies in Frankfurt and independently in the Soviet Union led to new insights and full theoretical clarification of the strong field problem [39].

4.1 — *The Decay of the Vacuum*

The decay of the vacuum in strong electrostatic fields is a relative recently recognized phenomenon in quantum electrodynamics that can be studied only via low-energy heavy-ion collisions. The original motivation for developing the new concept of a charged vacuum arose in 1965-70 in connection with understanding the atomic structure of superheavy nuclei expected to be produced by the GSI-heavy ion linear accelerator.

The best starting point for discussing this concept is to consider the binding energy of atomic electrons as the charge of a heavy nucleus is increased. In view of the large mass of the heavy nucleus compared to the electron mass, the external field approximation is quite appropriate. Solving the Dirac equation in the presence of an electromagnetic field gives the well-known fine

structure formula, first derived by Sommefeld from the early theory of the atom:

$$E(nj) = m_0c^2\left[1 + \left(\frac{Z\alpha}{n - |K| + \sqrt{K^2 - Z^2\alpha^2}}\right)^2\right]^{1/2} \qquad (1)$$

$n = 1, 2, \ldots\ldots\ldots\ldots$ = principal quantum number;
$K = \pm 1, \pm 2, \ldots\ldots\ldots\ldots$ = azimuthal quantum number;
$\alpha = e^2/c\hbar \ldots\ldots\ldots\ldots$ = fine-structure constant.

Because of the term $[K^2 - Z^2\alpha^2]^{1/2}$, equation (1) breaks down at $Z\alpha > |K|$. Thus all states with $j = 1/2$ cease to exist at $Z = 1/\alpha = 137$, as shown in Fig. 15: the corresponding wave function becomes non-normalizable at the origin; $E(1s_{1/2})$ becomes zero, i.e. the K-shell binding energy goes to $-m_0c^2$. Note from Fig. 15 that the energy levels move only very slowly away from the upper continuum as Z rises until $Z = 137$ is approached rather closely. Thus, even in the heaviest known element, the binding is only a small fraction of the rest energy.

The $Z = 137$ 'catastrophe' was well-known but it was argued loosely that it disappears when the finite size of the nucleus is taken into account. But Greiner and his coworkers showed that the problem is not removed but merely postponed and reappears at $Z \sim 173$; the exact value of this critical Z depends on many assumptions concerning the potential in the vicinity of the nucleus, in particular the nuclear radius. One can trace any level $E(nj)$ down to a binding energy of twice the electronic rest mass if the nuclear charge is increased as a parameter. At the corresponding charge number, which we shall call Z_{cr}, the state reaches the negative-energy continuum of the Dirac equation ('Dirac sea') which, according to the hole-theory hypothesis, is totally occupied by electrons. (The hole theory of Dirac is completely equivalent in its predictions to field theory). If the strength of the external field is further increased, the bound state dives into the continuum. The overcritical state acquires a width and is spread over the continuum. Still, the electron charge distribution does remain localized.

When Z exceeds 145, $E(1s_{1/2}) < 0$, i.e. the binding energy exceeds the rest mass of the electron. Adding the electron therefore diminishes the mass of the atom. It would be energetically advantageous for an electron to be spontaneously created, thereby

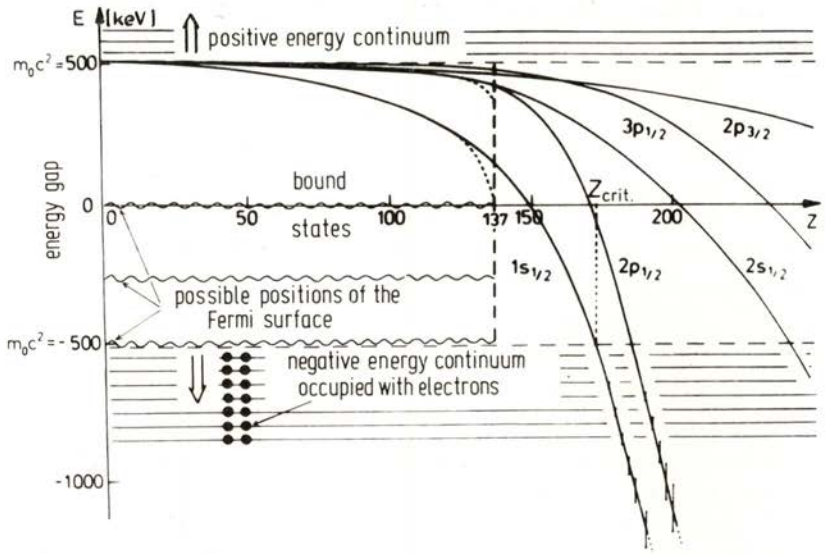

Fig. 15 — Lowest bound states of the Dirac-equation for nuclei with charge Z. While the Sommerfeld-eigenenergies (dashed lines) for $j = 1/2$ end at $Z = 137$ the solutions with extended Coulomb potential (full lines) can be traced down to the negative energy continuum which is reached at critical charge Z_{cr}. The states entering the continuum obtain a spreading width as indicated by the bars (magnified by a factor of 10). If the state was previously unoccupied two positrons will be emitted spontaneously.

reducing the total energy. This is not possible because it would violate the conservation of charge and lepton number. Similarly, when $Z > Z_{cr}$ a K-shell eletron is bound by more than twice its rest mass, so that it becomes energetically favorable to create an electron-positron pair. Now, however, the spontaneous appearance of such a pair is not forbidden by any conservation law. The electron becomes bound in the $1s_{1/2}$ orbital and the positron escapes.

We say that the overcritical vacuum state is charged. This has the following meaning. As already stated, within the hole theory, which is a lucid model for interpreting the field theoretical (quantum electrodynamical) calculations, the states of negative energy are occupied with electrons. This was postulated by Dirac to avoid the decay of electronic states with emission of an infinite amount of energy. In the undercritical situation we can define a

vacuum state $|0>$ without charges or currents by choosing the Fermi surface (up to which the levels are occupied) below the lowest bound state: we set $E_F = -m_0 c^2$. The negative-energy continuum states occupied with electrons represent the model for this vacuum; its infinite charge is renormalized to zero, and so it is a *neutral* vacuum. If now an empty atomic state dives into the negative continuum, it will be filled spontaneously with an electron from the Dirac sea with the simultaneous emission of a free positron moving to infinity. The remaining electron cloud of the supercritical atom is necessarily negatively charged. Thus, the vacuum becomes *charged.*

An atom with $Z > 173$ and an empty K-shell will spontaneously shield itself by two K-electrons and emit two positrons of rather well-defined energy. This two-electron state becomes the stable state, and it forms in a time scale of about 10^{-20} sec. If the central charge is further increased to $Z = 184$ (diving point of the $2p_{1/2}$ level), the vacuum acquires a charge of -4e. With increasing field strength, more and more electronic bound states join the negative continuum, and each time the vacuum undergoes a new phase transition and becomes successively higher charged: the vacuum sparks in overcritical fields.

Clearly, the charged vacuum is a new ground state of space and matter. The normal, undercritical, electrically neutral vacuum, is in overcritical fields no more stable: it decays spontaneously into the new stable but charged vacuum. Thus the standard definition of vacuum, "a region of space without real particles", is not true in very strong external fields. It must be replaced by the new and better definition, the "energetically deepest and stable state that a region of space can have while being penetrated by certain fields" (see Fig. 16).

4.2 — *Superheavy Quasimolecules in Heavy-Ion Scattering*

Inasmuch as the formation of a superheavy atom of $Z > 173$ is very unlikely, a new idea is necessary to test these predictions experimentally. That idea, based on the concept of nuclear molecules was put forward by Greiner and co-workers in 1969: a *superheavy quasimolecule* forms temporarily during the slow collision of two heavy ions.

It will be sufficient to form the quasimolecule for a very short instant of time, comparable to the time scale for atomic processes to evolve in a heavy atom, which is typically of the order 10^{-18} - 10^{-20} sec. Consider the case where a U ion is shot at

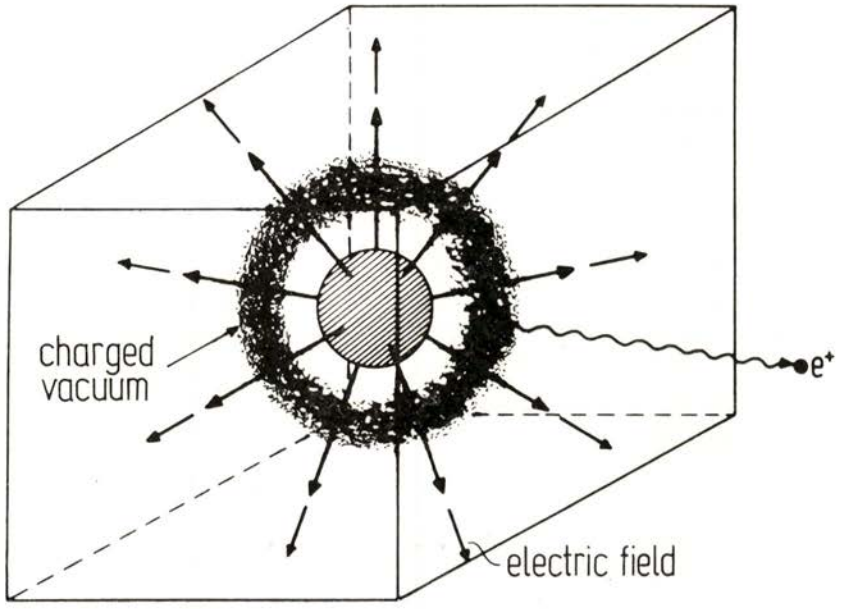

Fig. 16 — In overcritical fields space becomes charged through the emission of antiparticles. In principle the vacuum is no longer empty under these conditions. The shaded sphere in the center represents the superheavy nucleus, the source of the electric field indicated by arrows; the diffuse cloud represents the electrons of the charged vacuum. If this electron cloud is pumped away, new positrons (represented by e^+) will be emitted and the cloud will reappear. Hence under the extreme conditions of supercritical fields the vacuum is no longer empty: the vacuum is sparking.

another U ion at an energy corresponding to their Coulomb barrier and the two, moving slowly (compared to the K-shell electron velocity) on Rutherford hyperbolic trajectories, are close to each other (compared to the K-shell electron orbit radius). The two ions can be brought together as close as 20 fm for a time of ~ 10^{-21} sec. Then the atomic electrons move in the combined Coulomb potential of the two nuclei, thereby experiencing a field

corresponding to their combined charge of 184 (Fig. 17). This happens because $v_{ion} \sim c/10$, $v_{el} \sim c$: the ionic velocity is much smaller than the orbital electron velocity, so that there is time for electronic molecular orbits to be established while the two ions are in the vicinity of each other.

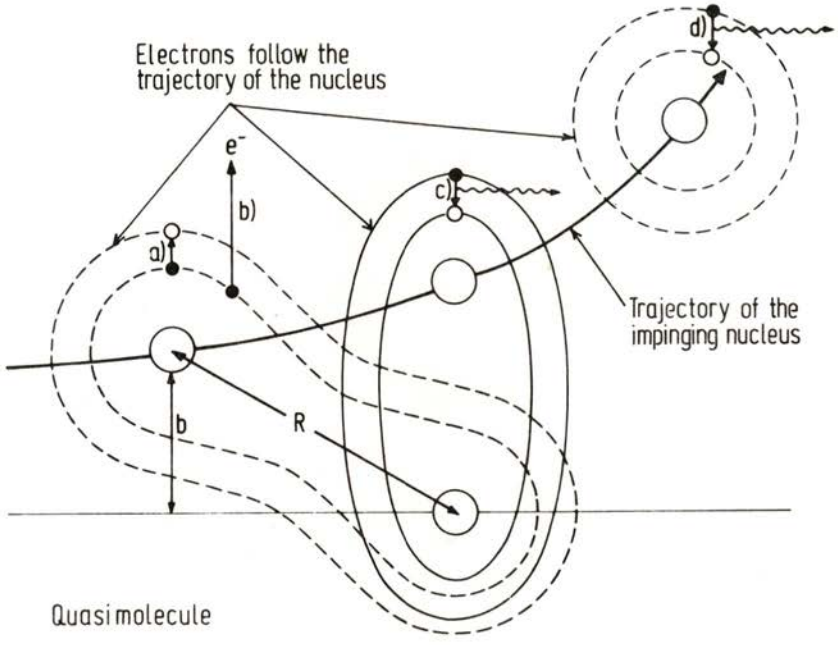

Fig. 17 — The basic concept concerning the formation of quasi molecules is shown. In the collision of two heavy ions the inner electrons orbit both nuclei together. The electron orbits follow the motion of the nuclei. Both nuclei are shown and their paths are indicated. The distance of closest approach is called the impact parameter. Processes of type a) (excitations of electrons into higher shells) and of type b) (excitations of electrons into the upper continuum) empty the K-shell. Processes c) and d) indicate the molecular and atomic X-ray transitions, respectively. The molecular X-rays are emitted from the intermediate quasi molecule, while the atomic X-rays are emitted from the rearranged atom after the collision.

The condition $v_{ion}/v_{el} \sim 1/10$ is known as adiabaticity. It will not help to make v_{ion} even smaller such that complete adiabaticity is achieved: for it is a partial breakdown of adiabaticity that

makes the inner shells of the quasimolecule ionized, i. e., empty of electrons, which, as we saw earlier, is a necessary prerequisite for the emission of positrons and the accompanying filling of the inner shell with electrons as it dives into the negative continuum.

When the two U atoms are separated by a large distance, the $Z = 184$ system is undercritical (i.e., all levels are bound by less than $2m_0c^2$). It becomes overcritical at small R as the electrons experience the full combined charge. For the $1s_{1/2}$ level the critical separation occurs at $R_{cr} = 35$ fm. The diving is very steep as a function of R. The level energies change rapidly only in the last 150 fm of the approach to the quasimolecule. This steep diving is important for the production of K holes (see the schematic Fig. 17).

4.3 — *Dynamical Processes in Heavy-Ion Collisions*

Several dynamical processes contribute to the ionization of the inner shells and to the production of positrons in undercritical as well as overcritical systems. This is illustrated in Fig. 18 for a system that becomes overcritical at small distances. In processes *a*) and *b*) one has electron excitation and ionization. Process *c*) is the spontaneous filling of a previously produced vacancy when the level acquires a binding greater than $2m_0c^2$ and is the decay of the vacuum described earlier. Because of the lack of full adiabaticity, energy can be drawn from the nuclear motion to lead to filling of the hole even at distances larger than R_{cr}. This effect (*d*, *e*) may be called an *induced transition*, and its effect on positron production is twofold: it causes a washed-out threshold for the spontaneous positron production, and it greatly enhances the production cross section. *f*) is the direct pair production process, which we now proceed to discuss in more detail.

Whereas in ordinary pair production in a Coulomb scattering process a photon is exchanged between two hadrons only once, now there are multiple interactions with the joint Coulomb field of both nuclei. Because of the very strong field, the cross section for the pair production varies as $(Z_1 + Z_2)^{19}$, which means that about 19/2 (!) photons are exchanged. This behavior illustrates the nonperturbative character of this process, which (like the induced decay mechanism) overwhelms the spontaneous positron

production process. The pair production process *f*) can be interpreted as the shake-off of the vacuum polarization (VP) cloud.

It is clear that a K hole is needed for the production of positrons by either the spontaneous or the induced mechanisms. Since neither the projectile nor the target atom has a K hole to start with, it has to be produced dynamically via Coulomb excitation or ionization (processes *a* and *b* of Fig. 18) in the collision

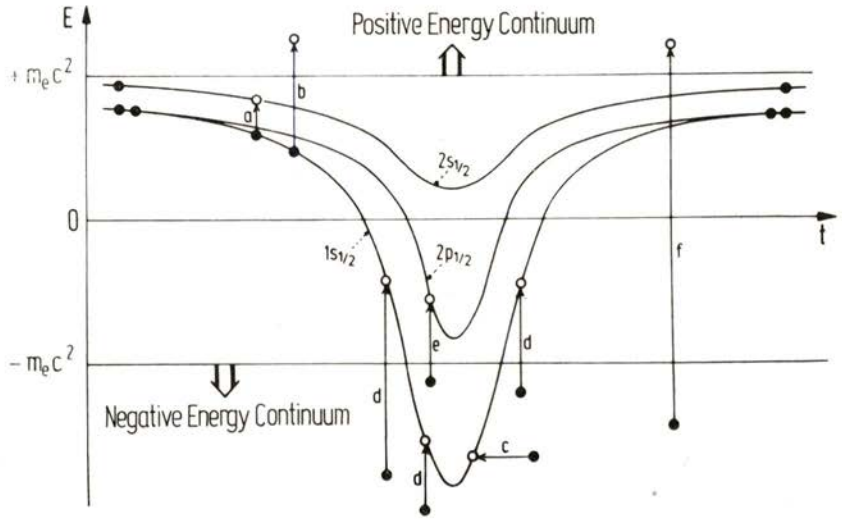

Fig. 18 — Dynamical processes connected with positron production in overcritical heavy-ion collisions. The figure shows the inner electron levels in the quasimolecule as a function of time. At the deepest point of the 1s level, the colliding nuclei are at the distance of closest approach.

a, b: electron excitation and ionization,
c: spontaneous autoionization of positrons,
d, e: induced decay of the vacuum,
f: direct pair creation.

itself. K-hole production occurs whenever the wavefunctions change so rapidly with R that the electrons can not adjust to the nuclear motion (breakdown of adiabaticity) and therefore get kicked out as δ electrons. Because of the rapid change of the wavefunctions at the onset of diving, vacancy production in the inner shell is concentrated at small values of R, which is advan-

tageous for the observation of induced and spontaneous positron emission.

The total K shell vacancy probability in the diving region for a U-U collision at an energy of 1600 MeV is predicted to be about 10 %, which is fully confirmed by recent experiments. [This includes both excitation and ionization, through one-step as well as multistep channels (see later)]. The other 90 % of the K electrons adjust to the nuclear motion, and hence the adiabaticity necessary for the theoretical treatment is generally valid.

The energy spectrum for positrons created in an e.g., Uranium-Uranium collision, consists of three components: the induced, the direct and the spontaneous one, which add up to a smooth spectrum. The presence of the spontaneous component leads

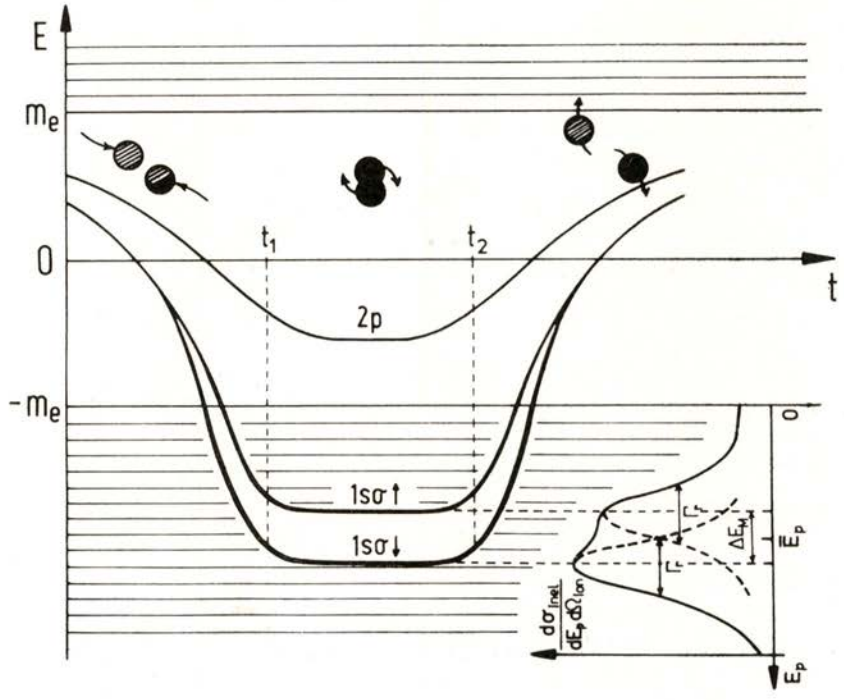

Fig. 19 — The innermost shells of the superheavy molecule (atom) as a function of time. Due to the sticking of the two nuclei, the superheavy atom lives for the time τ, thus being able to emit positrons spontaneously. There are in general two positron lines because of the Zeeman-splitting due to the strong magnetic fields from the heavy ion currents.

only to 5 - 10 % deviations for normal nuclear collisions along Rutherford trajectories. The question arises: Is there any way to get a clear qualitative signature for spontaneous positron production, as opposed to detecting it through a quantitative comparison with theory? Suppose that the two colliding ions, when they come close to each other, stick together for a certain time Δt before separating again. This will in general require the use of bombarding energies slightly above the Coulomb barrier. Then the quasimolecular levels in the overcritical region get stretched out as shown in Fig. 19 which is to be contrasted with Fig. 18. (The splitting in the energy of the $1s\sigma$ level arises from the Zeeman effect.) During the sticking, the energies of the electronic states do not change, and this has two effects: *a*) the emission of positrons from any given state occurs with a fixed energy; *b*) the induced production mechanisms do not contribute, whereas the spontaneous production (for overcritical states) continues to contribute.

The longer the sticking, the better is the static approximation. For Δt very long, one sees in the positron spectrum a very sharp line with a width corresponding to the natural lifetime of the resonant positron-emitting state (~ 3 keV for the U-U system). The observation of such a sharp line will not only indicate the spontaneous decay of the vacuum but also the formation of superheavy nuclear systems ($Z \gtrsim 180$) [40].

Naturally one is also interested in the question of what happens if the two nuclei stick, but for some yet unknown reason the $1s_{1/2}$ - level of an overcritical system does not dive, i.e., the neutral vacuum will not decay. Then an oscillatory structure as a function of the positron energy develops, which arises from the delayed interference between the incoming and the outgoing positron-creation-amplitudes along the trajectory of the colliding heavy ions. The positron spectrum will then have an oscillating structure as a function of positron energy from which the sticking time and even the structure (deformation, excited states) of the superheavy nuclear system can be deduced. In other words, we are dealing here with an *atomic clock* for short-living exotic nuclei. Because of the non-existence of a spontaneous amplitude in this case, the spontaneous positron emission line does not occur [40].

The search for spontaneous positron emission in heavy-ion collisions began in 1976 with the first acceleration of uranium

beams at Gesellschaft für Schwerionenforschung (GSI) in Darmstadt, West Germany. Experiments at this laboratory have utilized three detection systems, which have pursued complementary aspects of the problem [41-43]. We should note that in connection with these experiments it was necessary to establish that the conditions for forming quasimolecules could be met for the nuclear velocities required to achieve internuclear separations sufficiently small to produce overcritical binding. It was also critically important to demonstrate that the production probability for $1s\sigma$ vacancies was both large in magnitude and concentrated at small internuclear separations. There are several evidences for the formation of quasimolecules in heavy ion collisions such as δ electrons and molecular-orbital X rays (see review 38). Here we concentrate on the search for detection of spontaneous positron production.

One of the first experimental goals in the search for spontaneous positron emission was to determine the rate at which positrons are produced from the atomic processes relative to the rate at which they are produced from nuclear effects such as internal pair conversion of nuclear transitions. The first measurements [42] on the Pb^{208} - Pb^{208} collision system played a particularly important role in this respect and in confirming our theoretical understanding of the dynamic processes of positron production in heavy-ion collisions.

Measurements [43] on Pb-U and U-U collisions have carried these investigations into heavier systems, but under different and more complex background conditions. To investigate the consequences of this nuclear background in more detail, researchers carried out a systematic investigation of the ratio of positron intensity to γ - ray intensity over a broad range in Z. When Z_u, the combined nuclear charge $Z_1 + Z_2$, exceeds about 160, there is a spectacular increase in the total positron yield over that expected from nuclear internal pair conversion as it is extrapolated from the positron to γ-ray ratios measured for $Z_u < 160$. More precisely, for constant R_{min} and relative velocity, the production of positrons in superheavy collision systems is found to increase as $(Z_1 + Z_2)^{21}$. In this striking feature, which seems to have no other analog in nature, the theory [44] of dynamic positron creation in heavy-ion collisions again anticipated the experimental results.

The most recent experiments [45-48] have focussed on studying positron spectra and on extending the investigations to collision systems with higher total nuclear charge. With more comprehensive data, new phenomena have appeared that may be connected with the effects being sought. Of special interest are peak-like structures in the positron energy distribution. The most compelling evidence for these comes from experiments [45, 48] where coincidences between two scattered ions are used to define clearly events with two-body final states consistent with, or bordering on, elastic scattering. We illustrate these interesting results with an example.

The uranium-curium collision system, with $Z_u = 188$, has the largest combined nuclear charge investigated to date. Fig. 20 shows positron spectra from uranium-238 and curium-248 colliding at an energy close to that of the Coulomb barrier. Particularly striking in Fig. 20 is the well-defined peak centered at an energy of about 320 keV. The height of this peak above the smoother continuum is correlated with the choice of two-body final states corresponding to a selected range of scattering angles for the two heavy ions.

By comparison, if one singles out scattering angles more forward than those selected in Fig. 20 this peak is largely excluded. One finds a spectrum that mirrors the general shape of the continuum underlying the peak in Fig. 20. The continuum distributions are well represented by the spectra we expect [44] from the dynamically induced processes at the corresponding scattering angles. As we will see, it is also significant to find that the measured width of the peak in Fig. 20 is less than 100 keV. Moreover, this width is consistent with the Doppler broadening expected for a positron line spectrum emitted from a system moving with the velocity of the quasimolecular system. Therefore, the intrinsic width of the peak is surely less than 100 keV and, indeed, it could be very much smaller than this value.

Whatever the source of the peak, it is apparent that we must seek an explanation outside the scope of the theory based on Rutherford scattering alone, because this theory of dynamic positron creation does not allow for narrow peak structures in the positron spectrum. Deviations from this theory also have been demonstrated [45-47] for U-U collisions in other experiments

carried out at GSI. All experiments carried out to date indicate that there is a new source of positrons — a source that does not

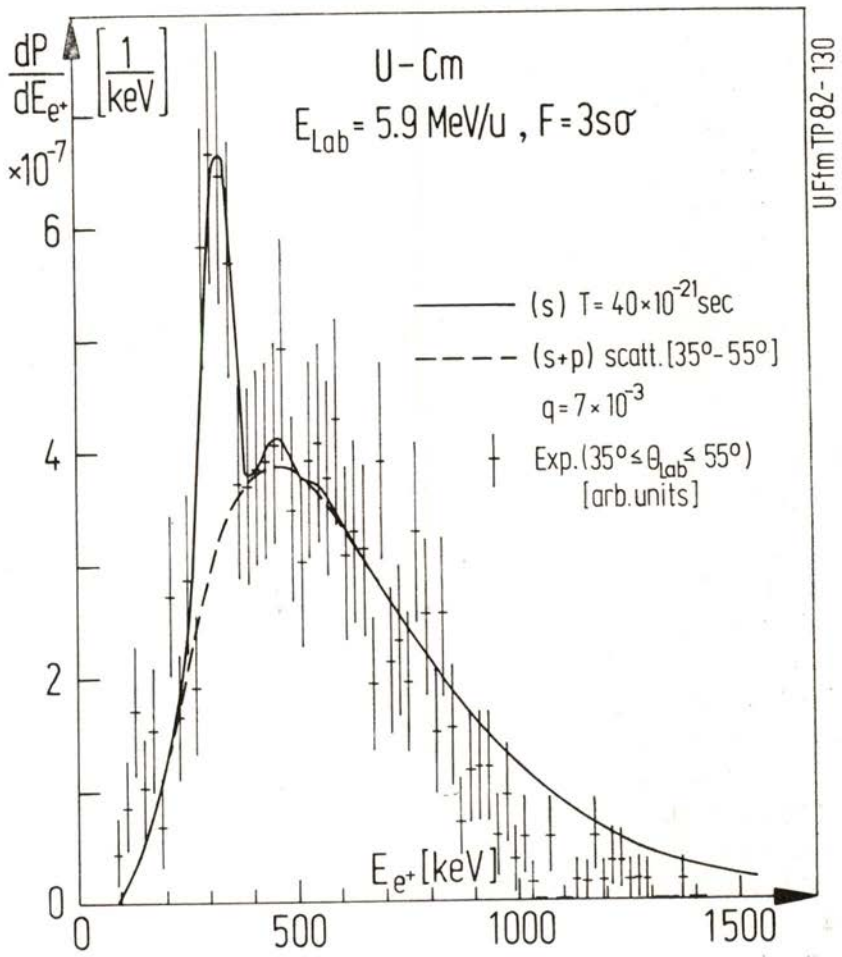

Fig. 20 — Positron spectra from 5.8 MeV/amu uranium-curium collisions. The full curve represents the theory. The line structure can only be understood, if a rather long-living (~ 10^{-19} sec) giant nucleus is formed.

originate with the known dynamic mechanisms associated in a simple way with the time-varying electric field produced in Coulomb trajectories.

It is also difficult to attribute these deviations from smooth positron spectra to pure nuclear effects. There are two prominent candidates:

— the internal pair conversion of a nuclear transition leading to a positron energy distribution that may be peaked,

— the internal pair conversion process followed by the capture of the electron into empty atomic orbits, which leads to positron line spectra.

The relatively narrow peak shapes that appear seem to preclude the former, while intensity considerations exclude the latter by orders of magnitude. But to exclude any connections with nuclear transitions, we need additional direct studies of these and other effects, and work is in progress toward this goal.

Of course, the observation of the U-Cm system's line-like positron spectrum, and the fact that it seems to appear only under particular scattering conditions, opens up to serious consideration the possibility that we may be observing the spontaneous emission of positrons. We are encouraged by the fact that this peak happens to occur at an energy consistent with a calculation [40] of the $1s\sigma$ resonance energy in the U-Cm quasiatom. Obviously, a systematic confirmation is required to follow up on these very suggestive data, but these new developments already raise the possibility of another important observation. For if the narrow positron peak does indeed represent spontaneous positron emission, the parent nuclear supercritical charge must exist for a long time compared to the collision times for scattering beneath the Coulomb barrier, as we pointed out earlier.

Therefore, Reinhardt, Müller, Müller and Greiner [40] suggested that the observation of spontaneous positron emission as a sharp line necessarily implies that, at bombarding energies close to that of the Coulomb barrier, a metastable superheavy nuclear composite system forms with a lifetime long enough to account for the relatively narrow peak. Widths of 100 keV or less correspond to lifetimes for the dinuclear system longer than about 40 times the Rutherford scattering collision time, during which the $1s\sigma$ state is overcritically bound. Indeed, without introducing a time delay it is difficult to invent any mechanism associated

with atomic positron emission that would explain the narrow peak width found in the U-Cm spectrum or the positron distribution emitted from the U-U collisions. Such a delay could be supplied by the formation of a rather cold intermediate superheavy nuclear complex as the nuclei barely touch in overcoming the Coulomb barrier.

Thus several independent measurements confront us with evidence that there are peak structures in the positron spectra of collision systems where the quasiatom can have overcritically bound electrons. We are left with the task of identifying unambiguously the sources for these structures among the possibilities we have discussed.

Of course, identifying the spontaneous emission of positrons, and thereby obtaining the first observation of the spontaneous decay of the ground state in a fundamental field theory, is the primary goal of these investigations. But it would be also interesting to find that peaks in the positron spectra reflect nothing more than the interference of induced emission amplitudes, and thus, that overcritical binding does not occur in a situation where Dirac theory predicts that it should.

We have seen that nuclear time delay such as can be produced by the formation of giant metastable nuclei, could play a central role in demonstrating the sparking of the vacuum. Conversely, from the point of view of nuclear physics, we can use the peaks in the positron spectra as an atomic clock that indicates the existence of the superheavy nuclear system and provides a measure of its lifetime and properties. These experiments portend interesting and challenging research in the months and years to come.

5 — NEW NUCLEAR APPLICATIONS IN DIAGNOSTIC MEDICINE

The applications of knowledge and techniques from nuclear physics have grown by leaps and bounds since 1950. Here we want to emphasize two new applications: positron emission tomography, PET, and nuclear magnetic resonance, NMR, that may well revolutionize the field of medical imaging or diagnostic medicine in quality of detail and, with NMR, in safety of procedures

and in our ability to view even in dynamical situations the internal parts of our bodies.

Computer Assisted Tomography, CAT, scans already have made significant advances in medical imaging. It uses X-rays, a multi-array of nuclear detectors and sophisticated computer programs to give cross-sectional views of different parts of the body.

Now, in positron emission tomography, PET, cyclotrons are being used to extend this technique in important ways. Short lived radioactive isotopes of C, N, O which emit positrons, are produced in a cyclotron. One can label a particular molecule with such an isotope so it will go to a particular area of the patient. There, when the positron is emitted, it quickly is brought to rest and when that occurs it finds an electron and they annihilate each other with all their mass emitted as two γ rays. These γ rays are emitted back to back exactly 180° with respect to each other. By detecting these γ rays in coincidence, one can tell very precisely the location of their emission. Fig. 21 shows a cross section of a brain taken with a PET system to study the visual response of the brain. When vision occurs, glucose metabolism occurs. By taking different slices through the visual cortex one can map out the performance of every part. Similar studies can be made of the functioning of other parts of brain or body. While the differences in Fig. 21 are much clearer when color is used to define different parts and different activities such as glucose metabolism, the effects can be seen in Fig. 21. The visual cortex is seen at the lowest, central part of the Figure as shown by the central arrow. On the right when no vision is occurring, no glucose metabolism is occurring. On the left, the gray center in the somewhat rectangular light area (in color the gray is red and the light area yellow) indicates glucose metabolism is taking place. From such pictures, one can see how well all parts are functioning at each level.

The development of nuclear magnetic resonance for medical imaging is the key to a major revolution in diagnostic images. The concept of using NMR techniques in tumor detection was first introduced by Ramon Damadian in 1971, when quantitative NMR parameters were measured and found to be different in solid malignant tumors than in normal tissues. A review of this field is given by Partain et al. [49] in a book on the *Physical Basis of Medical Imaging*.

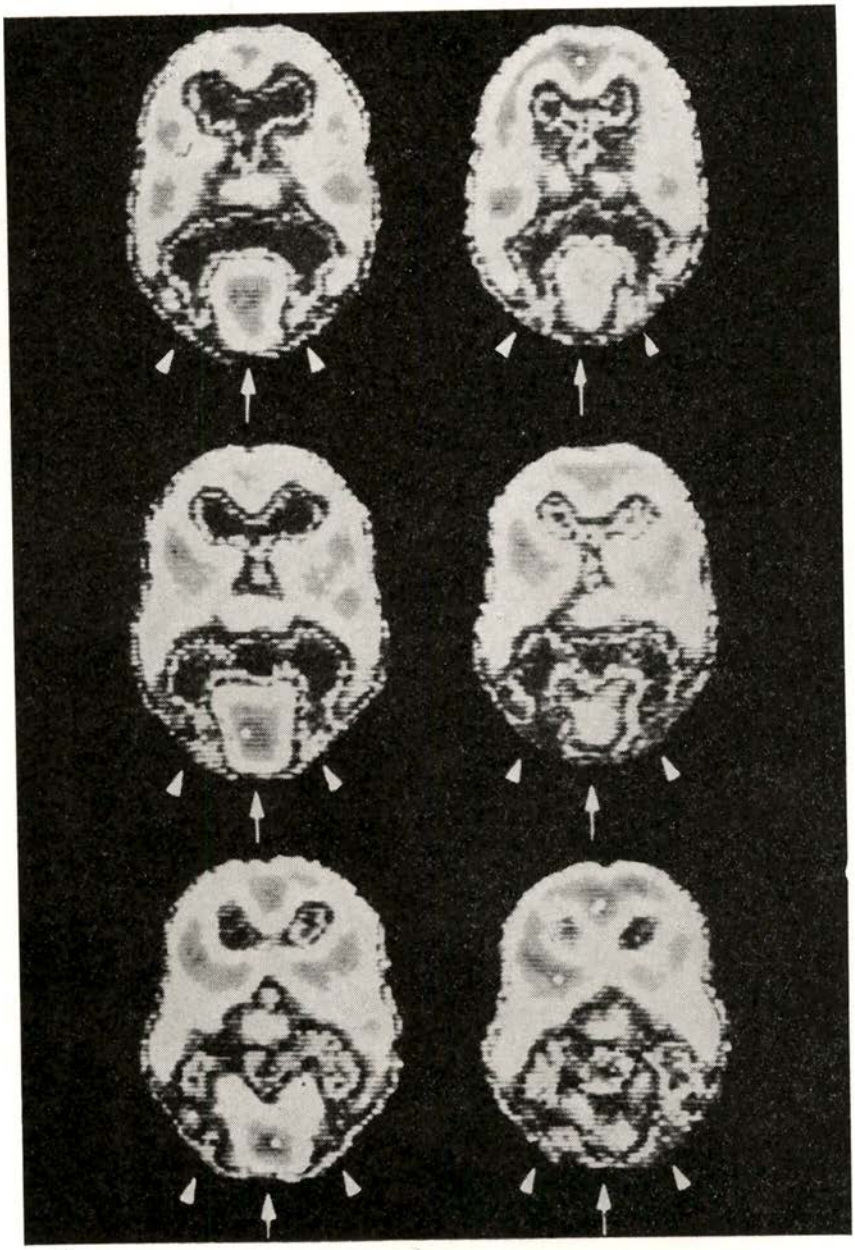

Fig. 21 — Cross section of a brain taken at three different levels with PET. On the left are shown three cross sections taken while vision is occurring, and on the right when the eyes were closed.

We will not here review NMR techniques. Suffice it to show how NMR can be used with a patient (Fig. 22). In Fig. 23 is shown a view of the head of Dr. Partain from Vanderbilt taken by an

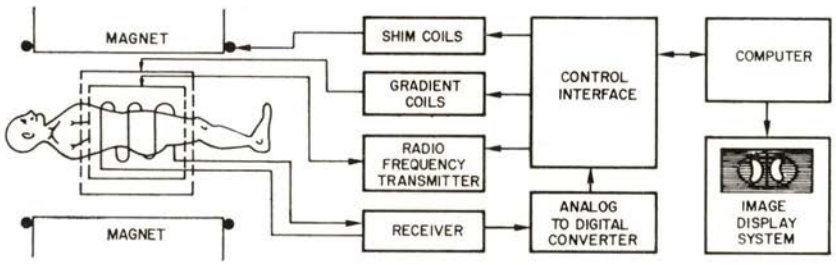

Fig. 22 — A schematic drawing of an NMR system for diagnostic imaging.

NMR system in England in early 1981. Even in this very early research-state facility, one can see details that show the exciting promise of this technique.

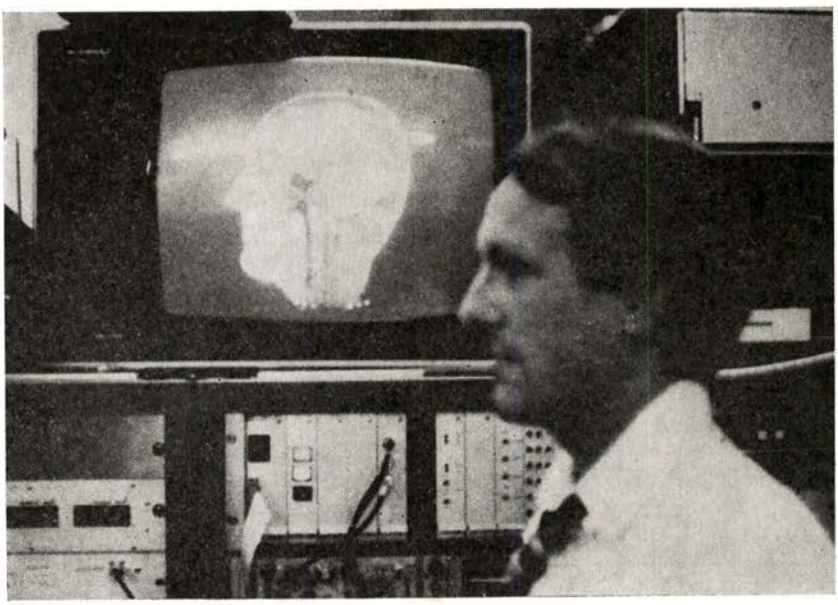

Fig. 23 — An NMR image of the head of Dr. Partain is seen on the screen. Dr. Partain is seen standing in front of the screen. The picture was taken in England.

The great interest in NMR imaging is because NMR is non-ionizing, noninvasive, without known risk, and in addition allows tomographic imaging based on the chemistry and metabolism within thin sections. That is, one does not use X- or γ-rays or radioactive materials which may have harmful side effects. Moreover, one can study dynamical effects, the actual working efficiency of an organ or component because of the dependence of NMR on the chemical state and metabolism taking place. This would include blood flow and organ motion in addition to simply identifying deseased tissue as distinguished from normal tissue. It is apparent that NMR imaging is developing into a technique of major importance in medical diagnosis and biochemical research. A tremendously bright future for NMR in medicine is seen.

We wish to thank our many colleagues for permission to use the results of their research. A special thanks is given Dr. Partain in Nuclear Medicine at Vanderbilt for the figures and discussions for the final section. Work at Vanderbilt University is supported in part by the U.S. Department of Energy, under Contrat No. DE-AS05-76ER05034.

REFERENCES

[1] A. BOHR and B. R. MOTTELSON, *Dan. Mat. Fys. Medd.*, **27** (1953), No. 16; *Alpha-, Beta- and Gamma-Ray Spectroscopy*, K. Siegbahn, ed., (North Holland Publ. Co., Amsterdam, 1955), p. 468.

[2] J. H. HAMILTON, A. V. RAMAYYA, E. L. BOSWORTH, W. LOURENS, J. D. COLE, B. VAN NOOIJEN, G. GARCIA-BERMUDEZ, B. MARTIN, B. N. SUBBA RAO, H. KAWAKAMI, L. L. RIEDINGER, C. R. BINGHAM, F. TURNER, E. F. ZGANJAR, E. H. SPEJEWSKI, H. K. CARTER, R. L. MLEKODAJ, W. D. SCHMIDT-OTT, K. R. BAKER, R. W. FINK, G. W. GOWDY, J. L. WOOD, A. XENOULIS, B. D. KERN, K. J. HOFSTETTER, J. L. WEIL, K. S. TOTH, M. A. IJAZ, K. S. R. SASTRY, *Phys. Rev. Letts.* **35**, 562 (1975); J. D. COLE, J. H. HAMILTON, A. V. RAMAYYA, W. G. NETTLES, H. KAWAKAMI, E. H. SPEJEWSKI, M. A. IJAZ, K. S. TOTH, R. L. ROBINSON, K. S. R. SASTRY, J. LIN, F. T. AVIGNONE, W. H. BRANTLEY, P. V. G. RAO, *ibid.*, **37**, 1185 (1976).

[3] J. H. HAMILTON, *Proc. Int. Conf. on Selected Topics in Nuclear Structure*, ed., V. G. SOLOVIEV et al. (Dubna, USSR, 1972), vol. II, p. 303; J. H. HAMILTON, *Nukleonika*, **24**, 561 (1979).

[4] J. H. HAMILTON, A. V. RAMAYYA, W. T. PINKSTON, R. M. RONNINGEN, G. GARCIA-BERMUDEZ, R. L. ROBINSON, H. J. KIM, R. O. SAYER, H. K.

CARTER, *Phys. Rev. Lett.*, **32**, 239 (1974); J. H. HAMILTON et al., *ibid.*, **36**, 340 (1976).

[5] J. H. HAMILTON, R. L. ROBINSON, and A. V. RAMAYYA, in *Nuclear Interactions*, B. A. ROBSON, ed. (Springer Verlag, Berlin, 1979), pp. 253-268; *Phys. Energiae Fortis et Phys. Nuclearis*, **3**, 355 (1979) (in Chinese).

[6] A. P. DE LIMA, J. H. HAMILTON, A. V. RAMAYYA, B. van NOOIJEN, R. M. RONNINGEN, H. KAWAKAMI, R. B. PIERCEY, R. L. ROBINSON, H. J. KIM, W. K. TUTTLE, L. K. PEKER, F. A. RICKEY and R. POPLI, *Phys. Letters*, **83B**, 43 (1979); *Phys. Rev.*, **C23**, 213 (1981).

[7] M. VERGNES, *Structure of Medium-Heavy Nuclei*, ed. G. S. ANAGNOSTA, *Inst. Phys. Conf. Ser.*, **49**, 25 (1980).

[8] R. LECOMTE, G. KAJRYS, S. LANDSBERGER, P. PARADIS, S. MONARO, *Phys. Rev.*, **C25**, 2812 (1982).

[9] K. KUMAR, *J. Phys. G. Nucl. Phys.*, **4**, 849 (1978).

[10] R. B. PIERCEY, J. H. HAMILTON, R. SOUNDRANAYAGAM, A. V. RAMAYYA, C. F. MAGUIRE, X.-J. SUN, Z. Z. ZHAO, R. L. ROBINSON, H. J. KIM, S. FRAUENDORF, J. DÖRING, L. FUNKE, G. WINTER, J. ROTH, L. CLEEMANN, J. EBERTH, W. NEUMANN, J. C. WELLS, J. LIN, A. C. RESTER, and H. K. CARTER, *Phys. Rev. Lett.*, **47**, 1514 (1981); R. B. PIERCEY, A. V. RAMAYYA, J. H. HAMILTON, X.-J. SUN, Z. Z. ZHAO, R. L. ROBINSON, H. J. KIM and J. C. WELLS, *Phys. Rev.*, **C25**, 1941 (1982); Z. Z. ZHAO, X.-J. SUN, R. B. PIERCEY, J. H. HAMILTON, C. F. MAGUIRE, A. V. RAMAYYA, R. L. ROBINSON, H. J. KIM, and J. C. WELLS, *Phys. Energiae Fortis et Phys. Nuclearis*, **6**, 255 (1982) (in Chinese).

[11] P. MÖLLER and J. R. NIX, *Nucl. Chemistry Symp. on Nuclei Far From Stability* (March 1982), Am. Chem. Soc. 183rd National Meeting, Abstracts Nucl. 16.

[12] M. SEIWERT, J. A. MARUHN, W. GREINER and A. V. RAMAYYA, *Int. Symp. on Dynamics of Nuclear Collective Motion*, K. OGAWA and K. TANABE, eds., published by INS, Tokyo, Japan (1982), pp. 422-430.

[13] M. BARCLAY, L. CLEEMANN, A. V. RAMAYYA, J. H. HAMILTON, J. D. COLE, A. P. DE LIMA, W. C. MA, S. C. PANCHOLI, R. SOUNDRANAYAGAM, H. YAMADA, W. ELLERBY, R. L. ROBINSON and W. MILNER, private communication (Fall 1981).

[14] M. BARCLAY et al., private communication, Vanderbilt University (Spring 1982).

[15] J. C. LISTER, B. J. VARLEY, H. G. PRICE and J. W. OLNESS, *Phys. Rev. Lett.*, **49**, 308 (1982).

[16] N. SAKAMOTO, S. MATSUKI, K. OGINO, Y. KADOTA, T. TANABE and Y. OKUMA, *Phys. Lett.*, **83B**, 39 (1979).

[17] G. WINTER, J. DÖRING, L. FUNKE, P. KEMNITZ and E. WILL, *Int. Symp. on Dynamics of Nuclear Collective Motion*, K. OGAWA and K. TANABE, eds., published by INS, Tokyo, Japan (1982), *Contributed Papers*, p. 21.

[18] R. B. PIERCEY et al., private communication, Vanderbilt University.

[19] L. FUNKE, G. WINTER, J. DÖRING, F. DUBBERS, P. KEMNITZ and E. WILL, *Future Directions in Studies of Nuclei Far From Stability*, eds. J. H. HAMILTON et al., North Holland Publ. Co. (1980), p. 231.

[20] R. E. AZUMA, G. L. BORCHERT, L. C. CARRAZ, P. G. HANSEN, B. JONSON, S. MATTSSON, O. B. NIELSEN, G. NYMAN, I. RAGNARSSON and H. L. RAVN, *Phys. Lett.*, **86B**, 5 (1979).

[21] H. WOLLNIK, F. K. WOHN, K. D. WÜNSCH and G. JUNG, *Nucl. Phys.* **A291**, 355 (1977).

[22] F. SCHUSSLER, J. A. PINKSTON, E. MONNAND, A. MOUSSA, G. JUNE, E. KOGLIN, B. PFEIFFER, R. V. F. JANSSENS and J. VAN KLINKEN, *Nucl. Phys.* **A339**, 415 (1980).

[23] J. C. HILL, K. SHIZUMA, H. LAWIN, M. SHAANAH, H. A. SELIČ and K. SISTEMICH, *IV Int. Conf. on Nuclei Far From Stability*, CERN 81-09 (1981), p. 443.

[24] K. SISTEMICH, W. D. LAUPPE, H. LAWIN, H. SEYFART and B. D. KERN, *Z. Physik*, **A289**, 225 (1979).

[25] A. BOHR and B. R. MOTTELSON, *Nuclear Structure*, vol. 2 (Benjamin, NY, 1975).

[26] R. S. SIMON et al., *Int. Symp. on Dynamics of Nuclear Collective Motion*, K. OGAWA and K. TANABE, eds., published by INS, Tokyo, Japan, (September 1982), p. 35; and M. JÄÄSKELÄINEN et al., *Int. Symp. on Dynamics of Nuclear Collective Motion*, K. OGAWA and K. TANABE, eds., published by INS, Tokyo, Japan (1982), p. 51.

[27] I. Y. LEE, M. M. ALEONARD, M. A. DELEPLANQUE, Y. EL-MASRI, J. O. NEWTON, R. S. SIMON, R. M. DIAMOND and F. S. STEPHENS, *Phys. Rev. Lett.*, **38**, 1454 (1977).

[28] L. L. RIEDINGER, O. ANDERSEN, S. FRAUENDORF, J. D. GARRETT, J. J. GAARDHØJE, G. B. HAGEMANN, B. HERSKIND, Y. V. MAKOVETZKY, J. C. WADDINGTON, M. GUTTORMSEN and P. O. TJØM, *Phys. Rev. Lett.*, **44**, 568 (1980).

[29] H. YAMADA et al., to be published; and H. YAMADA and J. H. HAMILTON, *Int. Symp. on Dynamics of Nuclear Collective Motion*, K. OGAWA and K. TANABE, eds., published by INS, Tokyo, Japan (1982), p. 23.

[30] J. BURGE, E. L. DINES, S. SHIH, R. M. DIAMOND, J. E. DRAPER, K. H. LINDENBENGER, C. SCHÜCK and F. S. STEPHENS, *Phys. Rev. Lett.*, **48**, 530 (1982).

[31] J. ROTH, L. CLEEMANN, J. EBERTH, T. HECK, W. NEUMANN, M. NOLTE, R. B. PIERCEY, A. V. RAMAYYA and J. H. HAMILTON, in *Proc. of. IV Int. Conf. on Nuclei Far From Stability*, CERN 81-09 (1981), p. 680.

[32] J. ROTH, L. CLEEMANN, J. EBERTH, A. V. RAMAYYA, R. B. PIERCEY, J. H. HAMILTON, to be published; and J. H. HAMILTON et al., *Proc. IV Int. Conf. on Nuclei Far From Stability*, CERN 81-09 (1981), p. 391.

[33] D. L. SASTRY, A. AHMED, A. V. RAMAYYA, R. B. PIERCEY, H. KAWAKAMI, R. SOUNDRANAYAGAM, J. H. HAMILTON, C. F. MAGUIRE, A. P. DE LIMA, S. RAMAVATARAM, R. L. ROBINSON, H. J. KIM, J. C. WELLS, *Phys. Rev.*, **C23**, 2086 (1981).

[34] H. P. HELLMEISTER, U. KAUP, J. KEINONEN, K. P. LIEB, R. RASCHER, R. BALLINI, J. DELAUNAY and H. DUMONT, *Phys. Lett.*, **85B**, 34 (1979); *Nucl. Phys.*, **A332**, 241 (1979).

[35] H. YAMADA, C. F. MAGUIRE, J. H. HAMILTON, A. V. RAMAYYA, D. C. HENSLEY, M. L. HALBERT, R. L. ROBINSON, F. E. BERTRAND and R. WOODWARD, *Phys. Rev.*, **C24**, 2565 (1981).

[36] S. FRAUENDORF, *Phys. Scri.*, **24**, 349 (1981).

[37] W. GREINER and J. H. HAMILTON, *American Scientist*, **19**, 154 (1980).

[38] J. S. GREENBERG and W. GREINER, *Phys. Today*, **35** (8), 24 (1982).

[39] Review articles by: B. MÜLLER, *Ann. Rev. Nucl. Sci.*, **26**, 351 (1976); J. REINHARDT, W. GREINER, *Rep. Prog. Phys.*, **40**, 219 (1977); J. RAFELSKI, L. FÜLCHER, A. KLEIN, *Phys. Rep.*, **38C**, 227 (1978); S. J. BRODSKY, P. J. MOHR, in *Structure and Collisions of Ions and Atoms*, I. A. SELLIN, ed., (Springer-Verlag, NY, 1978), p. 3.

[40] J. REINHARDT, U. MÜLLER, B. MÜLLER and W. GREINER, *Z. Physik*, **A303**, 173 (1981).

[41] See talks by P. KIENLE, H. BACKE, H. BOKEMEYER and conference summary by J. S. GREENBERG in *Proc. of NASI Conf. on the Quantum Electrodynamics of Strong Fields*, Lahnstein/Rhein, W. GREINER, ed. (Plenum, NY, 1981); J. S. GREENBERG in *Electronic and Atomic Collisions*, N. ODA, K. TAKAYANAGI, eds. (North Holland, Amsterdam, 1980), p. 351; P. KIENLE in *Atomic Physics*, vol. 7, D. KLEPPNER, F. PIPKIN, eds. (Plenum, NY, 1981), p. 1.

[42] H. BACKE, L. HANDSCHUG, F. HESSEBERGER, E. KANKELEIT, L. RICHTER, F. WEIK, R. WILLWATER, H. BOKEMEYER, P. VINCENT, Y. NAKAYAMA, J. S. GREENBERG, *Phys. Rev. Lett.*, **40**, 1443 (1978).

[43] C. KOZHUHAROV, P. KIENLE, E. BEDERMANN, H. BOKEMEYER, J. S. GREENBERG, Y. NAKAYAMA, P. VINCENT, N. BACKE, L. HANDSCHUG, E. KANKELEIT, *Phys. Rev. Lett.*, **42**, 376 (1979).

[44] See reviews by U. MÜLLER, J. REINHARDT, T. DE REUS, P. SCHLÜTER, G. SOFF, K. H. WIETSCHORKE, B. MÜLLER, W. GREINER in *Proc. of NASI*

Conf. on the Quantum Electrodynamics of Strong Fields, Lahnstein/Rhein, W. GREINER, ed. (Plenum, NY, 1981).

[45] H. BOKEMEYER, K. BETHGE, H. FOLGER, J. S. GREENBERG, H. GREIN, A. GRUPPE, S. ITO, R. SCHULE, D. SCHWALM, J. SCHWEPPE, N. TRAUTMANN, P. VINCENT, M. WALDSCHMIDT, in *Proc. of NASI Conf. on the Quantum Electrodynamics of Strong Fields*, Lahnstein/Rhein, W. GREINER, ed. (Plenum, NY, 1981).

[46] H. BACKE, W. BONIN, E. KANKELEIT, M. KRÄMER, R. KRIEG, V. METAG, P. SENGER, N. TRAUTMANN, F. WEIK, J. B. WILHELMY, in *Proc. of NASI Conf. on the Quantum Electrodynamics of Strong Fields*, Lahnstein/Rhein, W. GREINER, ed. (Plenum, NY, 1981).

[47] P. KIENLE, in *Proc. of NASI Conf. on the Quantum Electrodynamics of Strong Fields*, Lahnstein/Rhein, W. GREINER, ed. (Plenum, NY, 1981).

[48] H. BOKEMEYER, K. BETHGE, H. FOLGER, J. S. GREENBERG, H. GREIN, A. GRUPPE, S. ITO, R. SCHULE, D. SCHWALM, J. SCHWEPPE, N. TRAUTMANN, P. VINCENT, M. WALDSCHMIDT, to be published.

[49] C. L. PARTAIN, R. R. PRICE, J. J. ERICKSON, J. A. PATTON, C. M. COULAM and A. E. JAMES, *The Physical Basis of Medical Imaging*, eds., C. M. COULAM, J. J. ERICKSON, F. D. ROLLO and A. E. JAMES (Appleton-Century-Crofts, NY, 1981), p. 243.